Regulation of outer kinetochore assembly during meiosis I and II by CENP-A and KNL-2/M18BP1 in C. elegans oocytes

Laura Bellutti, Nicolas Macaisne, Layla El Mossadeq, Thadshagine Ganeswaran, Julie C Canman, Julien Dumont

Article

Current Biology

Regulation of outer kinetochore assembly during meiosis I and II by CENP-A and KNL-2/M18BP1 in *C. elegans* oocytes

Graphical abstract

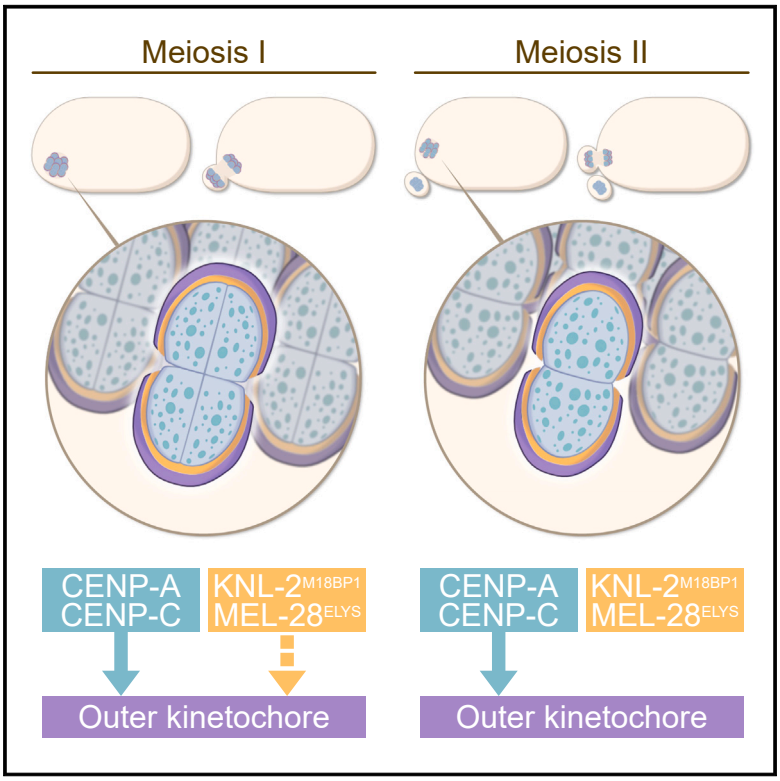

Authors

Laura Bellutti, Nicolas Macaisne, Layla El Mossadeq, Thadshagine Ganeswaran, Julie C. Canman, Julien Dumont

Correspondence

julien.dumont@ijm.fr

In brief

Bellutti et al. demonstrate that during meiosis I in *C. elegans* oocytes, outer kinetochore assembly relies on both the canonical CENP-A/C centromeric pathway and a parallel non-canonical KNL-2/MEL-28 pathway. By contrast, during meiosis II, outer kinetochore assembly depends solely on the CENP-A/C pathway.

Highlights

- CENP-A/C are essential for kinetochore assembly and function in meiosis I and II
- KNL-2/MEL-28 form a non-canonical kinetochore assembly pathway during meiosis I
- CENP-A/C and KNL-2/MEL-28 coordinate kinetochore assembly during meiosis I
- Kinetochore assembly is regulated differently between meiosis I and meiosis II

Bellutti et al., 2024, Current Biology *34*, 4853–4868
November 4, 2024
https://doi.org/10.1016/j.cub.2024.09.004

Current Biology

CellPress
OPEN ACCESS

Article

Regulation of outer kinetochore assembly during meiosis I and II by CENP-A and KNL-2/M18BP1 in *C. elegans* oocytes

Laura Bellutti,[1] Nicolas Macaisne,[1] Layla El Mossadeq,[1] Thadshagine Ganeswaran,[1] Julie C. Canman,[2] and Julien Dumont[1,3,4,*]

[1]Université Paris Cité, CNRS, Institut Jacques Monod, 75013 Paris, France
[2]Columbia University, Irving Medical Center, Department of Pathology and Cell Biology, New York, NY 10032, USA
[3]X (formerly Twitter): @IJMonod
[4]Lead contact
*Correspondence: julien.dumont@ijm.fr
https://doi.org/10.1016/j.cub.2024.09.004

SUMMARY

During cell division, chromosomes build kinetochores that attach to spindle microtubules. Kinetochores usually form at the centromeres, which contain CENP-A nucleosomes. The outer kinetochore, which is the core attachment site for microtubules, is composed of the KMN network (Knl1c, Mis12c, and Ndc80c complexes) and is recruited downstream of CENP-A and its partner CENP-C. In *C. elegans* oocytes, kinetochores have been suggested to form independently of CENP-A nucleosomes. Yet kinetochore formation requires CENP-C, which acts in parallel to the nucleoporin MEL-28^{ELYS}. Here, we used a combination of RNAi and Degron-based depletion of CENP-A (or downstream CENP-C) to demonstrate that both proteins are in fact responsible for a portion of outer kinetochore assembly during meiosis I and are essential for accurate chromosome segregation. The remaining part requires the coordinated action of KNL-2 (ortholog of human M18BP1) and of the nucleoporin MEL-28^{ELYS}. Accordingly, co-depletion of CENP-A (or CENP-C) and KNL-2^{M18BP1} (or MEL-28^{ELYS}) prevented outer kinetochore assembly in oocytes during meiosis I. We further found that KNL-2^{M18BP1} and MEL-28^{ELYS} are interdependent for kinetochore localization. Using engineered mutants, we demonstrated that KNL-2^{M18BP1} recruits MEL-28^{ELYS} at meiotic kinetochores through a specific N-terminal domain, independently of its canonical CENP-A loading factor activity. Finally, we found that meiosis II outer kinetochore assembly was solely dependent on the canonical CENP-A/CENP-C pathway. Thus, like in most cells, outer kinetochore assembly in *C. elegans* oocytes depends on centromeric chromatin. However, during meiosis I, an additional KNL-2^{M18BP1} and MEL-28^{ELYS} pathway acts in a non-redundant manner and in parallel to canonical centromeric chromatin.

INTRODUCTION

The faithful segregation of genetic material during cell division is essential to ensure the genomic integrity of cells, tissues, and organisms. In most eukaryotes, accurate chromosome segregation relies on chromosome attachment to spindle microtubules via multiprotein kinetochores.[1,2] The outer layer of the kinetochore, responsible for microtubule binding, primarily consists of the highly conserved KMN network, which is named after its constituent sub-complexes: Knl1c, Mis12c, and Ndc80c.[3–10] In the majority of species and cell types, outer kinetochore components are recruited on the centromeric chromatin, which is epigenetically defined by the centromeric-specific histone H3 variant centromere protein A (CENP-A).[11–16] Between the centromeric chromatin and the outer kinetochore, the constitutive centromere-associated network (CCAN) forms the inner kinetochore, composed of 16 CENP proteins organized into 5 subcomplexes (CENP-C, CENP-O/P/Q/U/R, CENP-L/N, CENP-H/I/K/M, and CENP-T/W/S/X).[17–20] Within the CCAN, CENP-C and CENP-T directly bind to and recruit the KMN network.[21–25] Thus, in most cases, disruption or depletion of upstream CENP-A leads to the loss of centromeres and kinetochores, resulting in chromosome missegregation, aneuploidy, and ultimately, cell death.

During DNA replication, CENP-A-containing nucleosomes are distributed between newly replicated chromatids and must subsequently be replenished to ensure the systematic and precise propagation of centromeric chromatin through successive cell cycles.[26,27] In vertebrates, assembly of new CENP-A nucleosomes requires the coordinated action of the hetero-octameric Mis18 complex (composed of two Mis18α, four Mis18β, and two M18BP1 proteins) and CENP-C.[28–33] The Mis18 complex and CENP-C bind to and recruit the CENP-A-specific histone chaperone, Holliday junction recognition protein (HJURP), which in turn loads new CENP-A nucleosomes at centromeres.[34,35]

C. elegans is a holocentric organism with diffuse kinetochores that share a similar, though overall simpler, composition compared with the monocentric vertebrate regional kinetochores.[36] The *C. elegans* genome contains two CENP-A paralogous genes: the

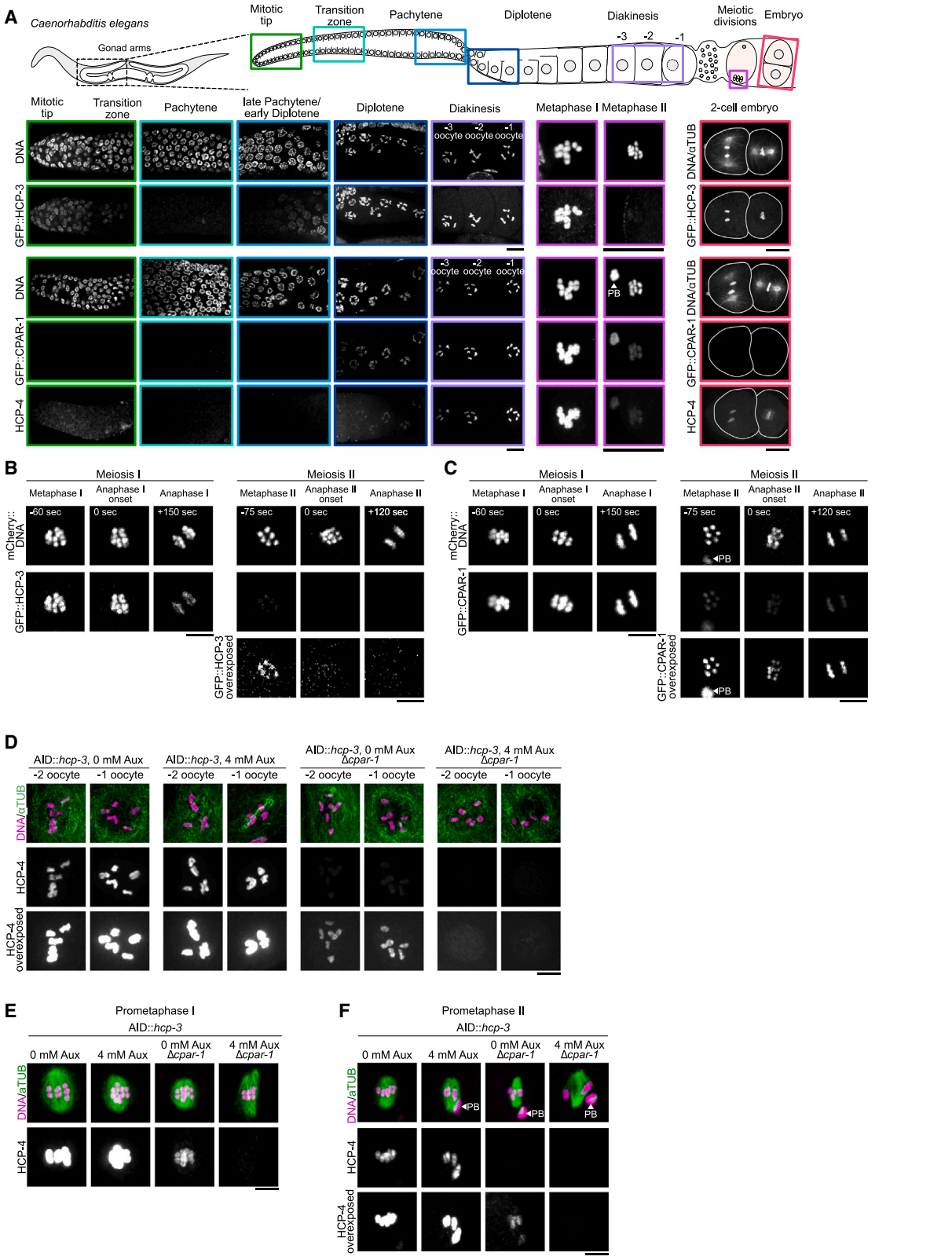

(legend on next page)

ubiquitously expressed HCP-3^{CENP-A} and a recent meiosis-specific duplication CPAR-1^{CENP-A}.[37,38] During mitosis in *C. elegans*, only HCP-3^{CENP-A} is present and necessary to assemble centromeric chromatin.[16,39] The incorporation of HCP-3^{CENP-A} into centromeric nucleosomes depends on the M18BP1 ortholog kinetochore-null (KNL)-2^{M18BP1}, which functions independently of Mis18 proteins that are not conserved in *C. elegans*.[29] KNL-2^{M18BP1} contains a conserved Myb-like (or SANT) DNA-binding domain and a SANT-associated (SANTA) domain whose functions are unclear. KNL-2^{M18BP1} displays two primary activities: first as a factor promoting chromosome condensation via a poorly characterized phospho-regulated C-terminal domain and second as a CENP-A loading factor via its middle unstructured region.[40,41] HCP-3^{CENP-A} and KNL-2^{M18BP1} interact directly through the CENP-A N-terminal tail and are mutually dependent for their centromeric localization.[40,42] Downstream of CENP-A, a simplified version of the CCAN, which consists solely of the CENP-C ortholog HCP-4^{CENP-C}, recruits the highly conserved KMN network to assemble the outer kinetochore.[43] In *C. elegans* embryos, the disruption of HCP-3^{CENP-A} or HCP-4^{CENP-C} completely abolishes outer kinetochore assembly and leads to the mitotic KNL phenotype, which corresponds to a complete failure to align chromosomes in metaphase and to segregate sister chromatids in anaphase.[6,39]

During oocyte meiosis in *C. elegans*, both centromeric histone H3 variants, HCP-3^{CENP-A} and CPAR-1^{CENP-A}, along with HCP-4^{CENP-C}, are present on chromosomes.[37,42,44] However, unlike outer kinetochore components, which concentrate on the outer surface of chromosomes to form cup-like holocentric meiotic kinetochores,[37,45–47] both CENP-A paralogs and the inner kinetochore protein HCP-4^{CENP-C} localize throughout chromatin.[37] Following nuclear envelope breakdown (NEBD) in meiosis I of *C. elegans* oocytes, most outer kinetochore components are also observed on filamentous structures known as linear elements, which are present in the cytoplasm and around the bivalent chromosomes but disappear abruptly at the onset of anaphase I.[37,48] Although the functional significance of these linear elements is unclear, they originate from the self-assembly of the outer kinetochore Rod-Zw10-Zwilch (RZZ) complex and are reminiscent of the kinetochore expansion observed at unattached vertebrate kinetochores.[49,50]

An initial study in *C. elegans* oocytes demonstrated that the two CENP-A paralogs, as well as HCP-4^{CENP-C}, are dispensable both for outer kinetochore assembly and chromosome segregation.[37] By contrast, more recent work revealed that HCP-4^{CENP-C} acts in parallel with the nucleoporin MEL-28^{ELYS} (see below) to promote outer kinetochore formation in *C. elegans* oocytes through a largely unknown mechanism.[51] Conclusions of these two studies present an apparent paradox, suggesting two possibilities: either HCP-4^{CENP-C} operates independently of CENP-A in defining and assembling outer kinetochores in *C. elegans* oocytes, or the role of CENP-A in this process has been previously overlooked.

The nucleoporin MEL-28^{ELYS} is the upstream component of the Y-complex, which together with 8 additional nucleoporins (NPP-2^{NUP85}, NPP-5^{NUP107}, NPP-6^{NUP160}, NPP-10C^{NUP96}, NPP-15^{NUP133}, NPP-18^{SEH1}, NPP-20^{SEC13R}, and NPP-23^{NUP43}) form the cytoplasmic and nucleoplasmic rings of nuclear pore complexes.[52–54] During meiosis, MEL-28^{ELYS} plays additional and antagonistic roles in oocytes: first, during prometaphase I, it promotes outer kinetochore assembly with HCP-4^{CENP-C}[51]; then, during anaphase I, it stimulates outer kinetochore disassembly by docking protein phosphatase I (PP1) at kinetochores.[55] Both functions of MEL-28^{ELYS} are essential for chromosome segregation in *C. elegans* oocytes. However, how MEL-28^{ELYS} is recruited to meiotic cup-like kinetochores and how it coordinates with HCP-4^{CENP-C} to concentrate outer kinetochore components there remains unknown.

To address these questions, we analyzed the localization dependencies and functions of both CENP-A paralogs, the inner kinetochore protein HCP-4^{CENP-C}, the CENP-A loading factor KNL-2^{M18BP1}, outer kinetochore components, and the nucleoporin MEL-28^{ELYS} during meiotic chromosome segregation using live and fixed *C. elegans* oocytes. We identify the unexpected and critical roles of HCP-3^{CENP-A} and CPAR-1^{CENP-A} in outer kinetochore assembly and ensuring the accuracy of meiotic chromosome segregation. Our results indeed highlight the differential requirement for CENP-A-containing centromeric chromatin in outer kinetochore assembly, which is essential in meiosis II but accounts for a portion of outer kinetochore formation in meiosis I. Additionally, we demonstrate that the atypical function of the nucleoporin MEL-28^{ELYS} in outer kinetochore assembly during meiosis I requires the coordinated function of KNL-2^{M18BP1}, with both proteins being mutually dependent for their cup-like kinetochore localizations. Finally, we identify an N-terminal domain of KNL-2^{M18BP1} responsible for this function, which operates independently of its canonical roles as a CENP-A loading factor and in promoting chromosome condensation.

RESULTS

HCP-3^{CENP-A} and CPAR-1^{CENP-A} act redundantly to recruit HCP-4^{CENP-C} on meiosis I chromosomes

We first analyzed the dynamic localization of endogenously GFP-tagged HCP-3^{CENP-A} and CPAR-1^{CENP-A} throughout the *C. elegans* germline (Figure 1A). In *C. elegans* hermaphrodites,

Figure 1. Dynamics of HCP-3^{CENP-A}, CPAR-1^{CENP-A}, and HCP-4^{CENP-C} during *C. elegans* female meiosis

(A) Top: schematic of an adult *C. elegans* hermaphrodite with a zoom on one gonad arm highlighting the different mitotic and meiotic stages. Bottom: immunofluorescence images of the different mitotic and meiotic stages within the germline and uterus in GFP::HCP-3^{CENP-A} and GFP::CPAR-1^{CENP-A}-expressing hermaphrodites immunostained for GFP, HCP-4^{CENP-C}, and DNA. The 2-cell stage embryos are also stained for α-tubulin (top). Scale bars, 10 μm.

(B and C) Representative time-lapse images of meiosis I and meiosis II of mCherry::HIS-11^{H2B} and GFP::HCP-3^{CENP-A} (B) or GFP::CPAR-1^{CENP-A} (C)-expressing control oocytes. Time in seconds relative to anaphase I onset (for meiosis I) or anaphase II onset (for meiosis II). White arrowheads indicate the first polar body (PB). Scale bar, 5 μm.

(D) Immunofluorescence images, centered on chromosomes, of oocytes in indicated conditions stained for α-tubulin (green), DNA (magenta), and HCP-4^{CENP-C} (gray). Scale bar, 5 μm.

(E and F) Immunofluorescence images, centered on the spindle, of oocytes during prometaphase I (E) and II (F) in indicated conditions stained for DNA (magenta), α-tubulin (green), and HCP-4^{CENP-C} (gray). White arrowheads indicate the first polar body (PB). Scale bar, 5 μm.

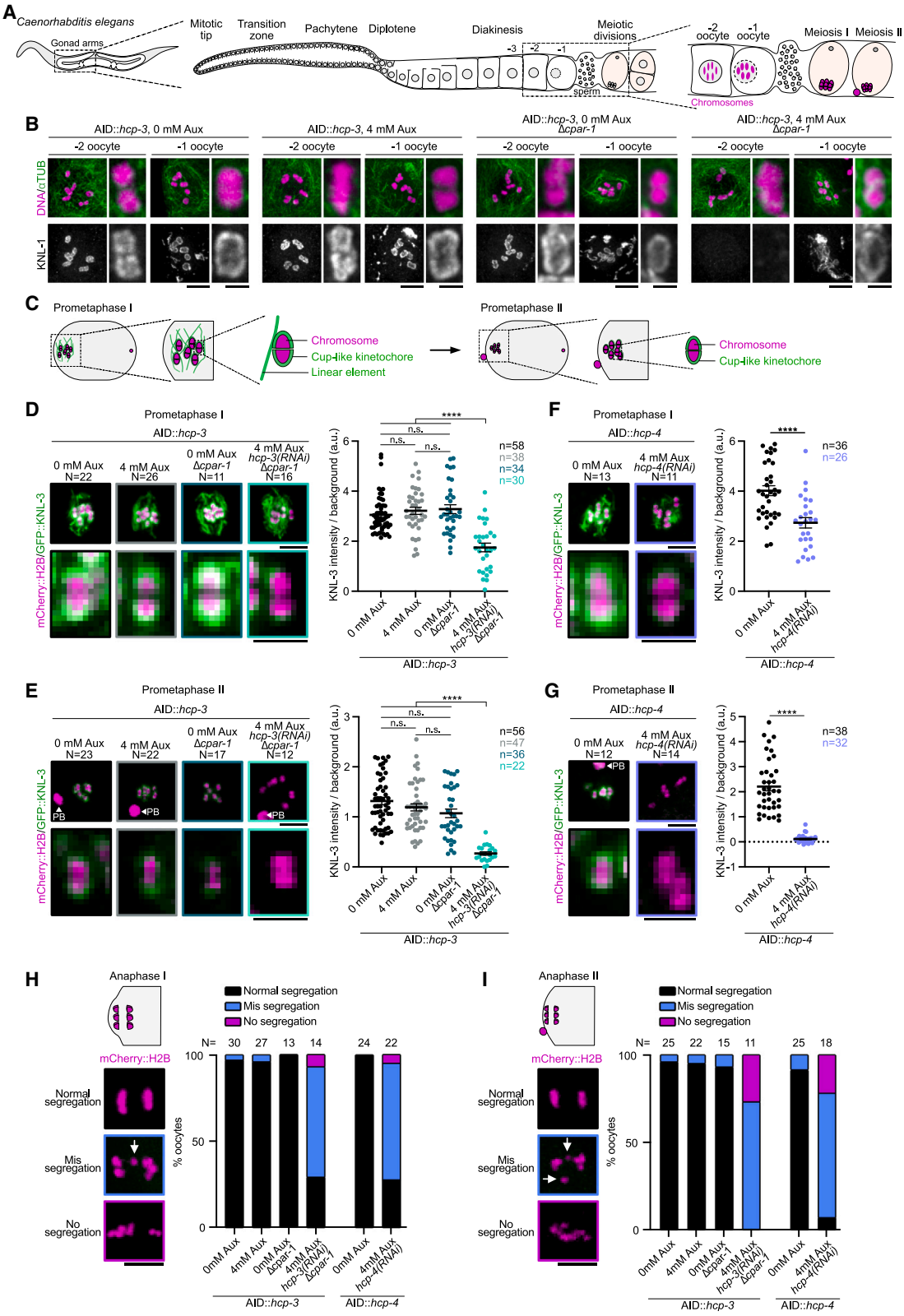

(legend on next page)

the germline is formed by two symmetrically folded arms. These are separated from a central uterus, which houses developing embryos, by two spermathecae (Figure 1A).[56] The distal-most part of the gonad arms contains mitotically dividing germline stem nuclei, which enter meiosis in the transition zone. Then, maturing oocytes progress proximally toward the spermathecae and undergo the two successive meiotic divisions after fertilization. In line with previous findings, we found that HCP-3^{CENP-A} was present throughout chromosomes at the mitotic tip and disappeared in the transition zone, only to reappear in early diplotene (Figure 1A).[44] By contrast, CPAR-1^{CENP-A} was initially absent from chromosomes, where it appeared at mid-diplotene. Both HCP-3^{CENP-A} and CPAR-1^{CENP-A} remained throughout chromatin during diakinesis and the first meiotic division (Figures 1A–1C). Their intensity was strongly reduced during meiosis II, and HCP-3^{CENP-A} even disappeared from chromosomes at anaphase II onset (Figures 1B and 1C). As expected, during mitosis in embryos, only HCP-3^{CENP-A} was present (Figure 1A).

In *C. elegans* mitosis, the only known inner kinetochore component HCP-4^{CENP-C} is recruited downstream of HCP-3^{CENP-A}.[39] Unlike CENP-C and other CCAN components that are constitutively present at centromeres in vertebrates, HCP-4^{CENP-C} is localized at centromeres exclusively during M-phase in *C. elegans*.[39] Accordingly, at the mitotic tip of the *C. elegans* germline, where most nuclei are in interphase, endogenously fluorescently tagged HCP-4^{CENP-C} did not concentrate on chromosomes but was instead faintly present in the cytoplasm (Figure 1A). It then appeared on chromosomes at mid-diplotene, paralleling the dynamic localization patterns of HCP-3^{CENP-A} and CPAR-1^{CENP-A} (Figure 1A).[37] Next, to determine the potential relationship between CENP-A and its partner protein CENP-C in the *C. elegans* germline, we analyzed the localization of HCP-4^{CENP-C} on chromosomes with or without HCP-3^{CENP-A} or CPAR-1^{CENP-A} (Figures 1D–1F). For this, we used CRIPSR-based genome engineering to generate a viable full deletion of *cpar-1^{cenp-a}* (Figure S1A), and we analyzed an auxin-inducible degradation (AID)-tagged allele of *hcp-3^{cenp-a}*.[42] HCP-4^{CENP-C} chromosomal intensity was unaffected by the depletion of HCP-3^{CENP-A} but was severely reduced in the absence of CPAR-1^{CENP-A} and undetectable upon depletion of both proteins during diakinesis and the two successive meiotic divisions. Thus, although both CENP-A paralogs appeared to act in parallel for the recruitment of HCP-4^{CENP-C} on chromosomes during diakinesis, CPAR-1^{CENP-A} exerted a dominant role.

HCP-3^{CENP-A}, CPAR-1^{CENP-A}, and HCP-4^{CENP-C} are differentially required during meiosis I and II for outer kinetochore assembly

We next reinvestigated the function of HCP-3^{CENP-A}, CPAR-1^{CENP-A}, and HCP-4^{CENP-C} in outer kinetochore assembly in the germline.[37] During mitosis, HCP-4^{CENP-C} plays a pivotal role in recruiting outer kinetochore components, including those belonging to the KMN network (Knl1c, Mis12c, Ndc80c), by interacting with multiple proteins within the heterotetrameric MIS12 complex (Mis12c composed of MIS-12^{MIS12}, KNL-3^{DSN1}, KBP-1^{NSL1}, and KBP-2^{PMF1}).[3,21,57] In control oocytes, KNL-1^{KNL1} and KNL-3^{DSN1} exhibited a dynamic localization pattern that evolved during diakinesis (Figures 2A, 2B, and S1B). Prior to NEBD (−2 oocyte), both proteins displayed a chromosomal localization, which subsequently concentrated at cup-like kinetochores following NEBD (−1 oocyte). At this stage, similar to most outer kinetochore components, they were also prominently enriched on linear elements (Figures 2B–2D, S1B, S1C, S1E, and S1F).[37,58] To test the potential roles of HCP-3^{CENP-A} and CPAR-1^{CENP-A} on KNL-1^{KNL1} and KNL-3^{DSN1} chromosomal or cup-like kinetochore localizations, we again used our full *cpar-1^{cenp-a}* deletion and the AID-tagged *hcp-3^{cenp-a}*.[42] We found that neither the auxin-induced degradation of HCP-3^{CENP-A} nor deleting *cpar-1^{cenp-a}* prevented endogenously GFP-tagged KNL-1^{KNL1} or KNL-3^{DSN1} localization on chromosomes during diakinesis (Figures 2B and S1B). However, the simultaneous absence of HCP-3^{CENP-A} and CPAR-1^{CENP-A} completely delocalized both proteins from chromosomes before NEBD (−2 oocyte). Despite this initial delocalization from chromosomes in the absence of both HCP-3^{CENP-A} and CPAR-1^{CENP-A}, we observed a sudden switch at NEBD when the two proteins accumulated at cup-like kinetochore structures and on linear elements (Figures 2B and S1B). Thus, after co-depletion of both HCP-3^{CENP-A} and CPAR-1^{CENP-A}, the downstream inner kinetochore component HCP-4^{CENP-C} was absent from chromosomes at NEBD (and throughout the two meiotic divisions) (Figures 1D–1F), yet the outer kinetochore proteins KNL-1^{KNL1} and KNL-3^{DSN1} were still present at cup-like kinetochores (Figures 2B and S1B).

Figure 2. Function of HCP-3^{CENP-A}, CPAR-1^{CENP-A}, and HCP-4^{CENP-C} in outer kinetochore assembly and chromosome segregation during female meiosis

(A) Left: schematic of an adult *C. elegans* hermaphrodite. Center: zoom on one gonad arm with the different stages of meiosis. Right: zoom on diakinesis oocytes and early embryos surrounding the spermatheca.

(B) Immunofluorescence images, centered on chromosomes, of oocytes in indicated conditions stained for DNA (magenta), α-tubulin (green), and KNL-1^{KNL1} (gray). Scale bars, 5 μm. For each condition and stage, a zoom on one pair of homologous chromosomes is shown on the right; scale bar, 1 μm.

(C) Schematic of outer kinetochore protein organization during prometaphase I and II. Outer kinetochore proteins localize at cup-like structures during meiosis I and II and at linear elements during meiosis I exclusively.

(D–G) Left: representative images of chromosomes in mCherry::HIS-11^{H2B} (magenta) and GFP::KNL-3^{DSN1} (green)-expressing oocytes in indicated conditions. White arrowheads indicate the first polar body (PB). Sample sizes (*N* oocytes). Scale bars, 5 μm. For each condition, bottom, zoom on one homologous chromosome pair (D and F) or on one sister chromatid pair (E and G); scale bars, 2 μm. Right: quantification of GFP::KNL-3^{DSN1} mean intensity at cup-like kinetochores. Error bars, SEM. Sample size (*n* cup-like kinetochores) is indicated for each condition. Kruskal-Wallis one-way ANOVA test (D and E) or Mann-Whitney test (F and G), ****$p < 0.0001$; n.s., not significant.

(H and I) Quantification of the percentage of oocytes showing normally segregating (gray), mis-segregating (blue), and non-segregating (violet) chromosomes during anaphase I (H) or anaphase II (I) in indicated conditions. Sample size (*N* oocytes) is indicated for each condition. White arrows indicate mis-segregating chromosomes. Scale bars, 5 μm.

See also Figures S1–S3 and Video S1.

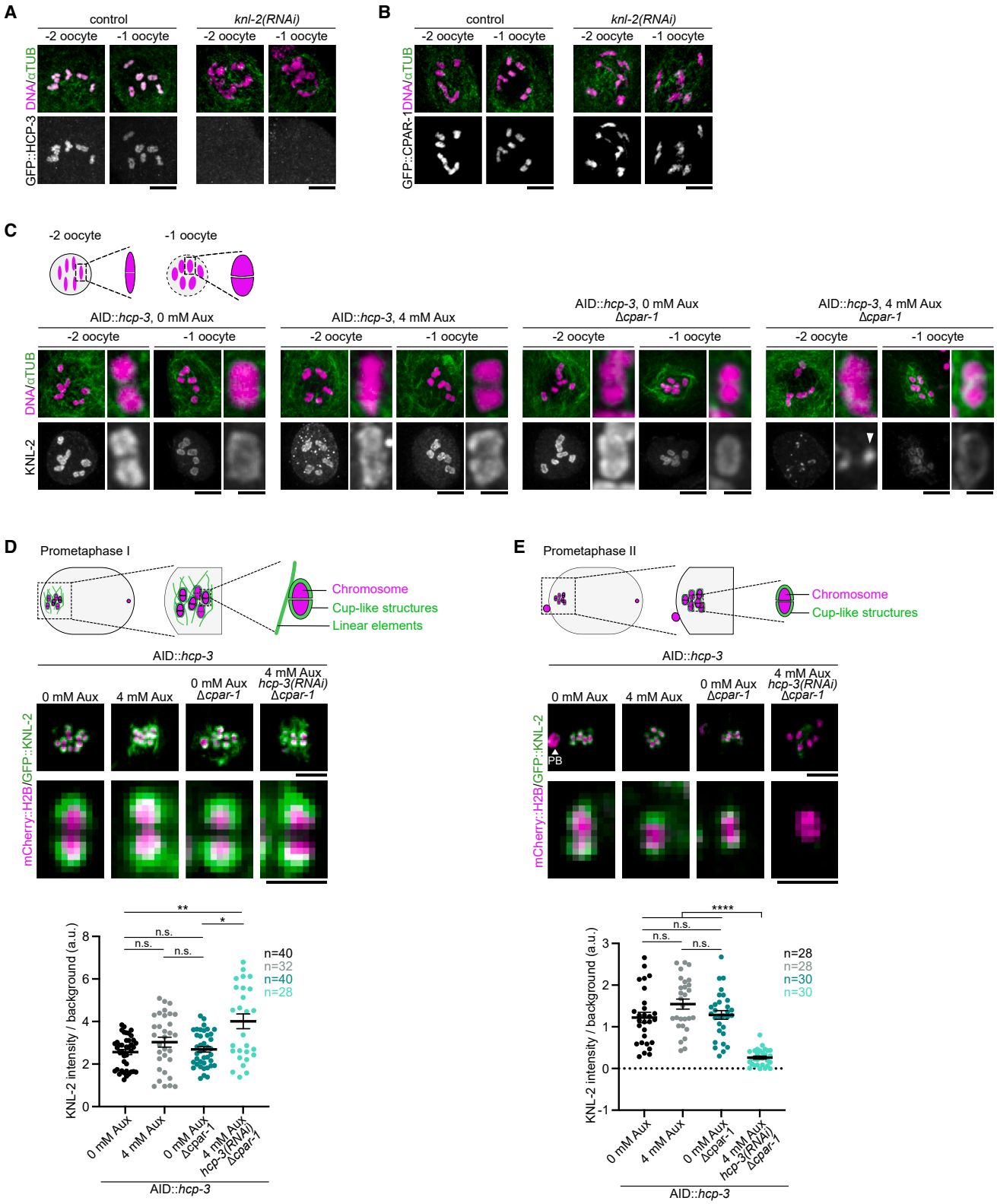

Figure 3. Functional relationship between HCP-3^{CENP-A}, CPAR-1^{CENP-A}, and KNL-2^{M18BP1} during female meiosis

(A and B) Immunofluorescence images, centered on chromosomes, of GFP::HCP-3^{CENP-A} (A) or GFP::CPAR-1^{CENP-A} (B)-expressing oocytes in indicated conditions stained for DNA (magenta), α-tubulin (green), and GFP (gray). Scale bars, 5 μm.

(legend continued on next page)

To functionally assess the apparent independence of outer kinetochore component cup-like localization with respect to HCP-3^{CENP-A}, CPAR-1^{CENP-A}, and HCP-4^{CENP-C}, we quantified the localization of endogenously GFP-tagged KNL-3^{DSN1} at cup-like kinetochores during prometaphase I and II in the presence or absence of the centromeric histone H3 variants and HCP-4^{CENP-C} (Figures 2D–2G).[59] Depleting or deleting either CENP-A paralog had no discernible effect on KNL-3^{DSN1} intensity at cup-like kinetochores during meiosis I or II (Figures 2D and 2E). By contrast, and to our surprise, the simultaneous absence of both HCP-3^{CENP-A} and CPAR-1^{CENP-A}, or the complete depletion of HCP-4^{CENP-C}, resulted in a strong reduction of GFP-tagged KNL-3^{DSN1} kinetochore intensity during meiosis I (42.7% and 31.9% mean intensity reduction in the absence of HCP-3^{CENP-A} and CPAR-1^{CENP-A}, or HCP-4^{CENP-C}, respectively; Figures 2D and 2F), and to its disappearance at kinetochores during meiosis II (79.7% and 94.9% mean intensity reduction in the absence of HCP-3^{CENP-A} and CPAR-1^{CENP-A}, or HCP-4^{CENP-C}, respectively; Figures 2E and 2G). By contrast, under these perturbed conditions, GFP-tagged KNL-3^{DSN1} did not appear to delocalize from the meiosis I-specific linear elements that normally surround the chromosomes at this stage (Figures 2D, 2F, S1E, and S1F). We importantly observed similar effects on GFP-tagged KNL-1^{KNL1} kinetochore localization upon HCP-4^{CENP-C} depletion (47.8% and 90.1% mean intensity reduction in the absence of HCP-4^{CENP-C} during meiosis I and II, respectively; Figures S1C and S1D).[59] This reduction or absence of KNL-1^{KNL1} and KNL-3^{DSN1} at kinetochores was concomitant with pronounced chromosome segregation defects, reminiscent of the meiotic KNL phenotype,[47,60,61] in meiosis I and II, respectively (Figures 2H, 2I, S1E, and S1F; Video S1). Furthermore, the meiosis II defects were not solely caused by prior meiosis I chromosome segregation errors. Specifically, 33% of HCP-3^{CENP-A} and CPAR-1^{CENP-A} co-depleted oocytes and 35% of HCP-4^{CENP-C}-depleted oocytes did not display any defects during meiosis I but exhibited severe chromosome segregation defects during meiosis II. Thus, during both meiosis I and II in *C. elegans* oocytes, the two CENP-A paralogs act in a parallel and partially redundant manner for outer kinetochore component cup-like localization and kinetochore-microtubule interaction. This function is tied to their role in recruiting HCP-4^{CENP-C} onto chromosomes, as depleting HCP-4^{CENP-C} led to identical results. However, although HCP-3^{CENP-A}, CPAR-1^{CENP-A}, and HCP-4^{CENP-C} were partially necessary during meiosis I, their strict requirement was observed during meiosis II. Overall, our results diverge from earlier studies that suggested a clear-cut independence between outer kinetochore component localization and kinetochore function with respect to CENP-A-containing centromeric chromatin and HCP-4^{CENP-C}.[37]

The three uncharacterized HFD proteins, F20D6.9, Y48E1C.1^{CENP-S}, and F35H10.5^{CENP-X}, do not participate in outer kinetochore assembly

Nevertheless, we observed the persistence of a significant amount of outer kinetochore components at cup-like kinetochores during meiosis I, even in the total absence of both CENP-A paralogs, or HCP-4^{CENP-C}. This prompted us to analyze the molecular mechanism accounting for the centromeric chromatin- and HCP-4^{CENP-C}-independent outer kinetochore assembly. We first examined the localization and potential function of three uncharacterized histone-fold domain (HFD)-containing proteins. These proteins could potentially bind to DNA independently of CENP-A and/or have been functionally linked to centromeres and kinetochores. The first protein, F20D6.9, is an atypical small histone H3 variant (Figure S2A). We identified two other proteins, Y48E1C.1 and F35H10.5, as potential orthologs of inner kinetochore components and CCAN proteins CENP-S and CENP-X, respectively (Figure S3A).[17,62–64] We generated transgenic *C. elegans* strains expressing GFP-tagged versions of the three proteins. While all three proteins were indeed expressed in the *C. elegans* germline and displayed a diffuse distribution within the nucleoplasm of diakinesis oocyte nuclei, none exhibited specific concentration on chromosomes or at cup-like kinetochores (Figures S2B, S3B, and S3C). Furthermore, by generating deletion mutants of the three candidate proteins using CRISPR-Cas9 genome editing, we observed that these mutants did not induce outer kinetochore defects on their own or when combined with the depletion or deletion of HCP-3^{CENP-A} and CPAR-1^{CENP-A} (Figures S2C and S3D–S3F). Altogether, these results suggest that F20D6.9, Y48E1C.1^{CENP-S}, and F35H10.5^{CENP-X} do not localize to nor contribute to the establishment of the outer kinetochore in *C. elegans* oocytes.

KNL-2^{M18BP1} localizes independently of HCP-3^{CENP-A} and CPAR-1^{CENP-A} at cup-like kinetochores during meiosis I

Another candidate protein, which potentially directly binds DNA through its MYB and SANTA domains and is functionally associated with centromeres and kinetochores, is the mitotic CENP-A-loading factor KNL-2^{M18BP1}.[29] During mitosis, HCP-3^{CENP-A} and KNL-2^{M18BP1} are mutually dependent for their centromeric localization.[29] We tested if this was also the case in the *C. elegans* germline. Depleting KNL-2^{M18BP1} by RNAi led to the expected chromosome condensation defects[29,41] and prevented HCP-3^{CENP-A} chromosomal localization during diakinesis and both meiotic divisions (Figures 3A and S4A). By contrast, CPAR-1^{CENP-A} was still present on chromosomes in the absence of KNL-2^{M18BP1} (Figures 3B and S4B). Thus HCP-3^{CENP-A}, but not CPAR-1^{CENP-A}, depends on KNL-2^{M18BP1} for its chromosomal

(C) Top: schematics of chromosomes in −2 and −1 oocytes. Bottom: immunofluorescence images, centered on chromosomes, of oocytes in indicated conditions stained for DNA (magenta), α-tubulin (green), and KNL-2^{M18BP1} (gray). Scale bars, 5 μm. For each oocyte, right: zoom on one homologous chromosome pair; scale bar, 1 μm. The white arrowhead indicates a KNL-2^{M18BP1} foci.

(D and E) Top: schematic of outer kinetochore protein organization during prometaphase I (D) and II (E). Middle: representative images of chromosomes in mCherry::HIS-11^{H2B} (magenta) and GFP::KNL-2^{M18BP1} (green)-expressing oocytes in indicated conditions. Scale bars, 5 μm. For each condition: zoom on one homologous chromosome pair (D) or on one pair of sister chromatids (E); scale bars, 2 μm. Bottom: quantification of GFP::KNL-2^{M18BP1} mean intensity at cup-like kinetochores. Error bars, SEM. Sample size (*n* cup-like kinetochores) is indicated for each condition. Kruskal-Wallis one-way ANOVA test, $^{*}p < 0.05$, $^{**}p < 0.01$, $^{****}p < 0.0001$; n.s., not significant.

See also Figure S4.

meiotic localization. KNL-2^{M18BP1} and HCP-3^{CENP-A} colocalize throughout the *C. elegans* germline.[42] However, while HCP-3^{CENP-A} is present throughout chromatin until the end of meiosis (Figure 1A), at NEBD during diakinesis (−1 oocyte) KNL-2^{M18BP1} started to concentrate at cup-like kinetochores (Figure 3C). We found that neither the auxin-induced degradation of HCP-3^{CENP-A} nor deleting *cpar-1^{cenp-a}* prevented KNL-2^{M18BP1} localization on chromosomes during diakinesis (Figure 3C). However, the simultaneous disruption of HCP-3^{CENP-A} and CPAR-1^{CENP-A} completely delocalized KNL-2^{M18BP1} from chromosomes before NEBD (−2 oocyte). Instead, KNL-2^{M18BP1} formed nucleoplasmic foci of unknown nature, some of which localized near chromosomes (Figure 3C). Unexpectedly, although KNL-2^{M18BP1} was initially absent from chromosomes in the absence of both HCP-3^{CENP-A} and CPAR-1^{CENP-A}, we observed a sudden switch at NEBD when KNL-2^{M18BP1} accumulated at cup-like kinetochore structures (Figure 3C). This cup-like localization of KNL-2^{M18BP1} persisted throughout meiosis I but strikingly disappeared upon entry into meiosis II when both histone H3 variants were absent (Figures 3D and 3E). In HCP-3^{CENP-A} and CPAR-1^{CENP-A} co-depleted oocytes, we also observed the presence of multiple KNL-2^{M18BP1} large aggregates at a distance from chromosomes during meiosis II, whose origin remains unclear (Figure 3E). Thus, while the chromosomal localization of KNL-2^{M18BP1} was initially and redundantly dependent on HCP-3^{CENP-A} and CPAR-1^{CENP-A}, its accumulation at cup-like kinetochores was independent of CENP-A-containing centromeric chromatin from NEBD until meiosis II onset.

KNL-2^{M18BP1} acts in parallel with HCP-3^{CENP-A} and CPAR-1^{CENP-A} for outer kinetochore assembly during meiosis I

The localization of KNL-2^{M18BP1} at cup-like kinetochores independently of both HCP-3^{CENP-A} and CPAR-1^{CENP-A} during meiosis I (Figure 3D) prompted us to analyze the potential contribution of KNL-2^{M18BP1} in centromeric chromatin-independent outer kinetochore assembly.[29,32,40,65,66] Upon KNL-2^{M18BP1} depletion, chromosomes exhibited evident condensation defects. However, GFP-tagged KNL-3^{DSN1} still localized, albeit at reduced levels, to misshaped cup-like structures during meiosis I (Figure 4A). In stark contrast, the simultaneous depletion of HCP-4^{CENP-C} and KNL-2^{M18BP1} completely prevented GFP-tagged KNL-3^{DSN1} localization at this stage (27.6% and 96% mean intensity reduction in the absence of KNL-2^{M18BP1} alone or in combination with HCP-4^{CENP-C} depletion, respectively; Figure 4A). Analyses during meiosis II yielded comparable results (97.1% mean intensity reduction in the absence of KNL-2^{M18BP1} and HCP-4^{CENP-C}; Figure 4B). However, the single depletion of KNL-2^{M18BP1} at this stage resulted in a more pronounced phenotype compared with its effect in meiosis I (73.8% mean intensity reduction in the absence of KNL-2^{M18BP1} alone; Figure 4B). Consistent with KNL-2^{M18BP1} being upstream of HCP-3^{CENP-A} for its chromosomal localization during meiosis I (Figures 3A and S4A), depleting KNL-2^{M18BP1} in CPAR-1^{CENP-A}-deficient oocytes was sufficient to prevent GFP-tagged KNL-3^{DSN1} from localizing to the outer kinetochores during meiosis I (77.8% and 90.1% mean intensity reduction in the absence of KNL-2^{M18BP1} and CPAR-1^{CENP-A} during meiosis I and II, respectively; Figures S4C and S4D). These results demonstrate that KNL-2^{M18BP1} acts coordinately with HCP-3^{CENP-A} and CPAR-1^{CENP-A}, and independently of its canonical CENP-A-loading factor activity, in outer kinetochore assembly during meiosis I in oocytes.

An N-terminal region of KNL-2^{M18BP1} is responsible for its kinetochore localization and its role in assembling the outer kinetochore

To determine the specific domain of KNL-2^{M18BP1} involved in meiosis I outer kinetochore assembly, we generated a series of KNL-2^{M18BP1} deletion mutants expressed as RNAi-resistant transgenes, and we analyzed their localization and function upon endogenous KNL-2^{M18BP1} depletion during metaphase I in *C. elegans* oocytes (Figure 4C). Consistent with KNL-2^{M18BP1} and CENP-A being mutually independent at this stage, deleting the CENP-A-interaction domain of KNL-2^{M18BP1} (amino acid [aa] 267–470) did not prevent kinetochore localization of the corresponding mutant upon endogenous KNL-2^{M18BP1} depletion. We obtained similar results upon removal of the MYB domain (aa 623–673) and/or the regions that surrounded it (aa 471–622 and 674–877). Conversely, the deletion of the SANTA domain (aa 2–113) or the region spanning from the SANTA to the CENP-A-interaction domains (aa 114–266) resulted in a significant reduction in the kinetochore localization of the respective mutants (Figure 4C). Deleting the SANTA domain did not fully prevent kinetochore localization, but removing the adjacent region (aa 114–266) or a larger fragment that included this region (aa 114–622) completely delocalized the corresponding mutant from kinetochores. Importantly, we checked that full-length and mutated transgenes were expressed at comparable levels (Figure S5A). Furthermore, upon co-depletion of endogenous KNL-2^{M18BP1} and the two CENP-A paralogs in this mutant (Δ114–266), mCherry-tagged KNL-1^{KNL1} was completely delocalized, while it was normally concentrated at cup-like kinetochores in all other mutants (Figure 4C). Thus, we identified an N-terminal region, distinct from the SANTA, CENP-A interaction, and MYB domains, responsible for KNL-2^{M18BP1} localization at cup-like kinetochores and essential for outer kinetochore assembly during meiosis I. We also observed that, despite not being localized on chromosomes, this N-terminal region mutant KNL-2^{M18BP1} (Δ114–266) supported normal chromosome condensation and did not exhibit the misshaped chromosomes typically observed upon KNL-2^{M18BP1} depletion (Figures 4C, S5B, and S5C).[29,41,42] Therefore, this mutant enabled a clear separation of KNL-2 functions in chromosome condensation and in assembly of the meiotic outer kinetochore. Overall, our results highlighted an unexpected meiosis I-specific function of KNL-2^{M18BP1} in outer kinetochore assembly in *C. elegans* oocytes, independent of its canonical activities as a CENP-A-loading factor or in controlling meiotic chromosome condensation.

KNL-2^{M18BP1} and MEL-28^{ELYS} cooperate for outer kinetochore assembly during meiosis I

Previous work has shown that, through an unknown mechanism, the Y-complex nucleoporin MEL-28^{ELYS} and HCP-4^{CENP-C} jointly regulate the recruitment of outer kinetochore components at cup-like kinetochores during meiosis I in *C. elegans* oocytes.[51] We confirmed these previous findings (95.7% and 99.3% mean intensity reduction in the absence of MEL-28^{ELYS} and

CellPress
OPEN ACCESS

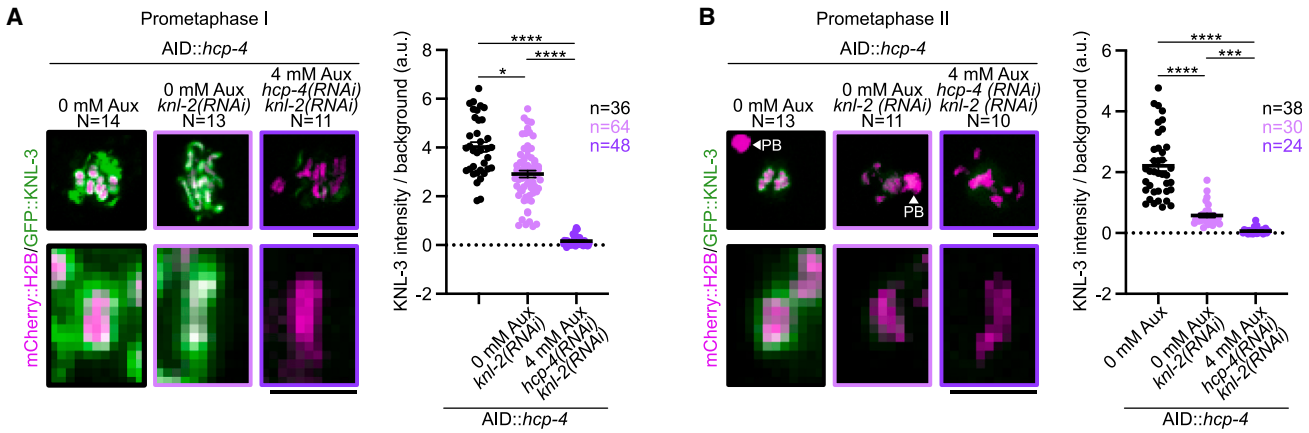

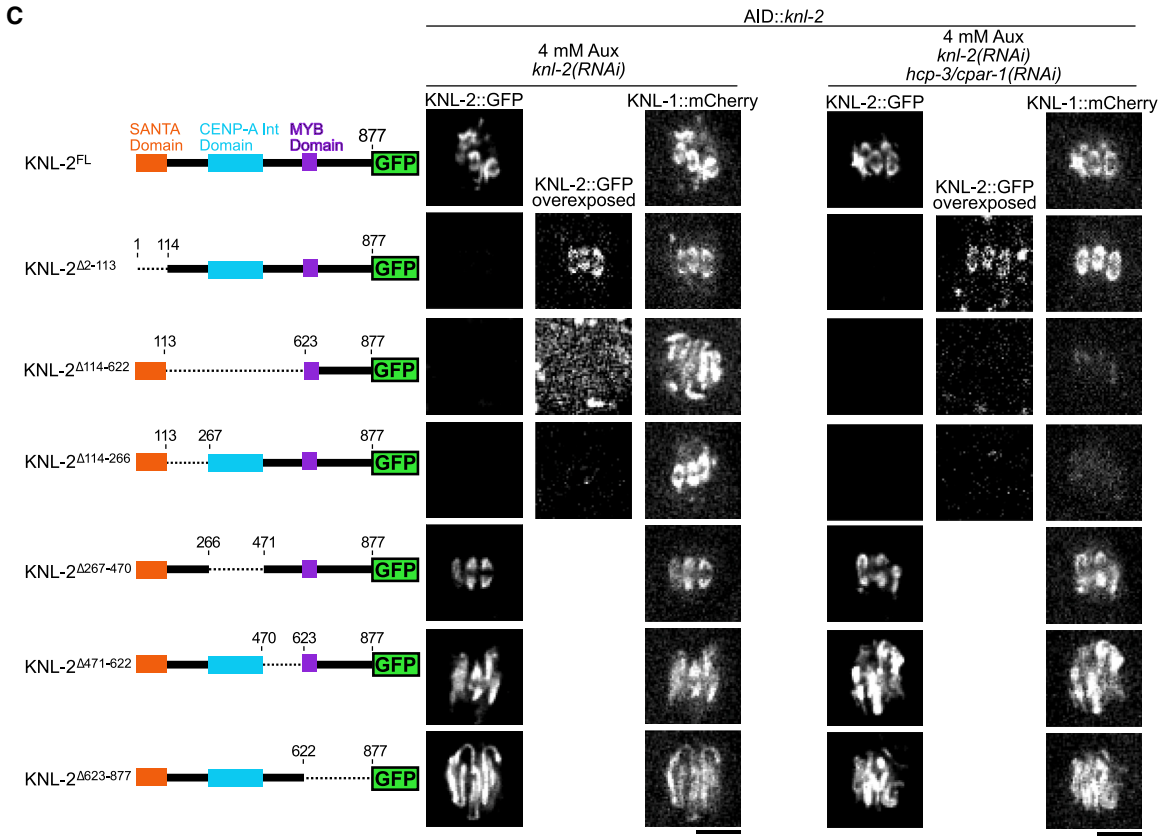

Figure 4. KNL-2^{M18BP1} and HCP-4^{CENP-C} act coordinately to assemble the outer kinetochore during meiosis I

(A and B) Left: representative images of chromosomes in mCherry::HIS-11^{H2B} (magenta) and GFP::KNL-3^{DSN1} (green)-expressing oocytes in indicated conditions. White arrowheads indicate the first polar body (PB). Sample sizes (*N* oocytes). Scale bar, 5 μm. For each condition, bottom: zoom on one homologous chromosome pair (A) or on one sister chromatid pair (B); scale bar, 2 μm. Right: quantification of GFP::KNL-3^{DSN1} mean intensity at cup-like kinetochores. Error bars, SEM. Sample size (*n* cup-like kinetochores) is indicated for each condition. Kruskal-Wallis one-way ANOVA test $^{*}p < 0.05$, $^{***}p < 0.001$, $^{****}p < 0.0001$.

(C) Left: schematics of truncated KNL-2^{M18BP1}::GFP transgenes used to identify functional domains for KNL-2^{M18BP1}::GFP and KNL-1^{KNL1}::mCherry localization at cup-like kinetochores. The deleted region is indicated with a dotted line on each schematic. Right: representative images of chromosomes in KNL-2^{M18BP1}::GFP and KNL-1^{KNL1}::mCherry-expressing oocytes in indicated conditions. Scale bar, 5 μm.

See also Figure S5.

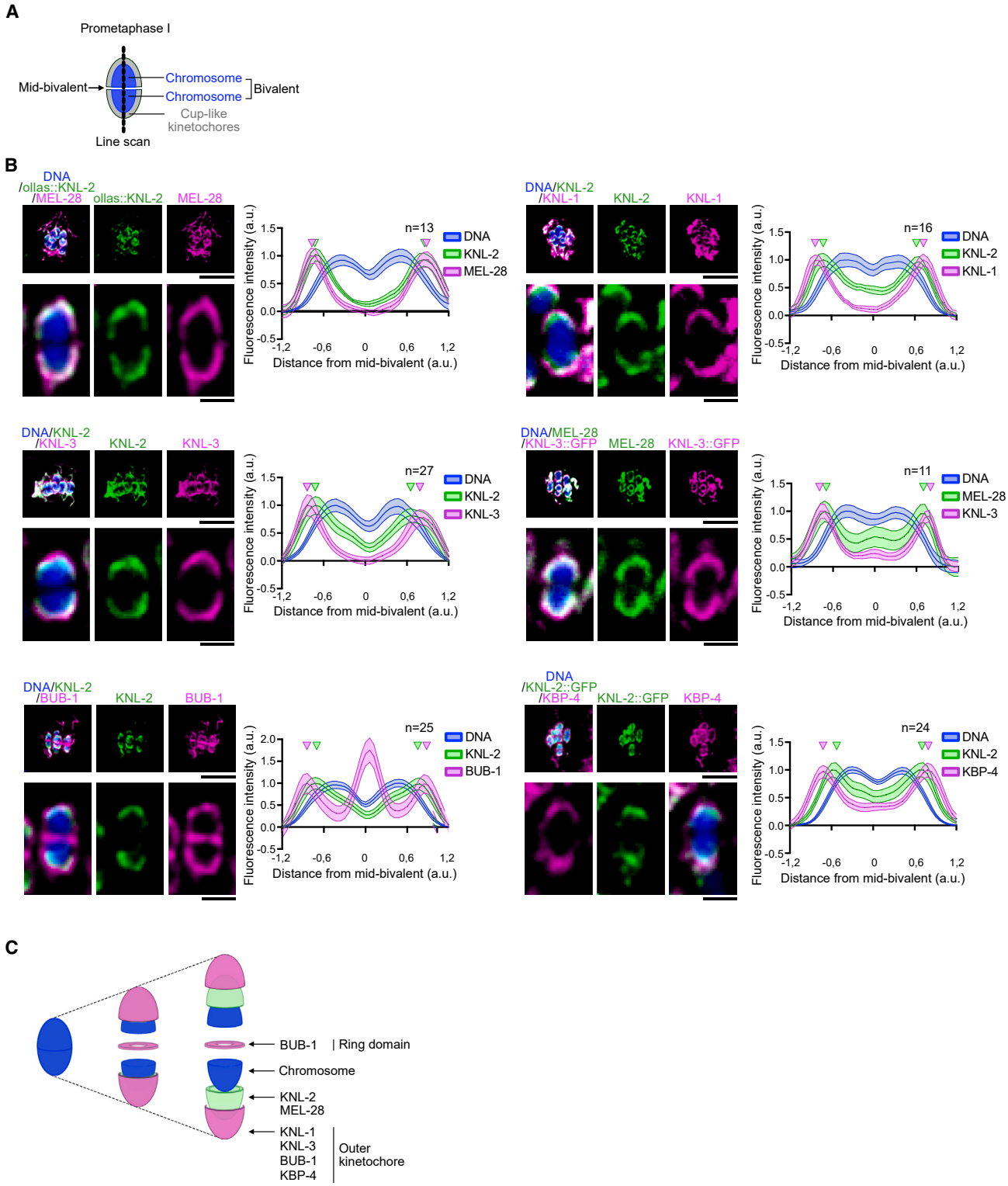

Figure 5. KNL-2^{M18BP1} and MEL-28^{ELYS} form cup-like structures internally to outer kinetochore proteins

(A) Schematic of one homologous chromosome pair (bivalent chromosome) and their cup-like kinetochores at prometaphase I. The dotted black line represents the line scan along each bivalent chromosome used to quantify the localization of MEL-28^{ELYS}, KNL-2^{M18BP1}, and outer kinetochore components at the cup-like structures.

(B) Immunofluorescence images of indicated kinetochore components during prometaphase I. For each condition, left top: image centered on the entire set of bivalent chromosomes, scale bar, 5 μm; left bottom: zoom on one homologous chromosome pair, scale bar, 1 μm; right: line scan quantifications of DNA (blue),

(legend continued on next page)

HCP-4^{CENP-C} during meiosis I and II, respectively; Figures S6A and S6B). Furthermore, our findings that KNL-2^{M18BP1} also functions in parallel with CENP-A and HCP-4^{CENP-C} in outer kinetochore assembly prompted us to explore the potential connection between KNL-2^{M18BP1} and MEL-28^{ELYS} in this process. We first confirmed that, like the other six Y-complex members, MEL-28^{ELYS} localized at cup-like kinetochores in *C. elegans* oocytes (Figures 5B, 6B, and S6E).[55] However, co-localization analysis of outer kinetochore components, MEL-28^{ELYS} and KNL-2^{M18BP1}, revealed that KNL-1^{KNL1}, KNL-3^{DSN1}, KBP-4^{SPC25} (component of the Ndc80c complex), and BUB-1^{BUB1} (component of the outer kinetochore BHC module)[58] formed wider cup-like structures, which surrounded MEL-28^{ELYS} and KNL-2^{M18BP1} (Figures 5B and 5C). By contrast, MEL-28^{ELYS} and KNL-2^{M18BP1} partially colocalized at internal cup-like structures, suggesting possible interaction between the two proteins (Figures 5B and 5C). We thus analyzed the potential relationship between KNL-2^{M18BP1} and MEL-28^{ELYS} for meiosis I outer kinetochore assembly. Depleting MEL-28^{ELYS} completely hindered the kinetochore localization of GFP-tagged KNL-2^{M18BP1} at the cup-like structures in both meiosis I and II (Figures 6A and S6C). This dependence was specific to the meiotic divisions, as during diakinesis, KNL-2^{M18BP1} relied on HCP-3^{CENP-A} and CPAR-1^{CENP-A} rather than on MEL-28^{ELYS}, for its chromosomal localization (compare the localization of KNL-2^{M18BP1} when MEL-28^{ELYS} and both CENP-A paralogs are co-depleted versus when MEL-28^{ELYS} and HCP-4^{CENP-C} are co-depleted; Figure S6D). By contrast, upon depletion of KNL-2^{M18BP1}, MEL-28^{ELYS} exhibited a faint but discernible localization at cup-like kinetochores (Figures 6B and S6E). The complete delocalization of GFP-tagged MEL-28^{ELYS} from kinetochores was observed only upon simultaneous depletion of KNL-2^{M18BP1} and of the two CENP-A paralogs (Figures 6B and S6E). This also differed from diakinesis, where the chromosomal localization of MEL-28^{ELYS} relied only on HCP-3^{CENP-A} and CPAR-1^{CENP-A} (Figure S6F). Additionally, analysis of the KNL-2^{M18BP1} deletion mutants, following depletion of HCP-3^{CENP-A} and CPAR-1^{CENP-A}, implicated the N-terminal region of KNL-2^{M18BP1} (aa 114–266), which we identified as essential for outer kinetochore assembly, in MEL-28^{ELYS} kinetochore localization (Figures 6C and S6G). Thus, while MEL-28^{ELYS} was strictly required for KNL-2^{M18BP1} kinetochore localization, CENP-A- (and CENP-C)-dependent centromeric chromatin cooperated with MEL-28^{ELYS} for KNL-2^{M18BP1} localization at cup-like kinetochores.

DISCUSSION

In conclusion, our findings identify three distinct meiotic phases for chromosomal localization of outer kinetochore components in *C. elegans* oocytes (Figure 6D). During the first phase spanning from early diakinesis to NEBD, the two CENP-A paralogs and their loading factor KNL-2^{M18BP1} are interdependent for their localization. They colocalize with downstream HCP-4^{CENP-C} and outer kinetochore components throughout chromosomes. The functional significance of this chromosomal localization of outer kinetochore components is unclear as microtubules are confined outside the nucleus and are thus distant from chromosomes at this stage. The second phase extends from NEBD until the onset of meiosis II when the last phase starts. While HCP-3^{CENP-A}, CPAR-1^{CENP-A}, and HCP-4^{CENP-C} maintain their chromosomal localization, other components become restricted at cup-like kinetochores during the meiotic divisions. Our results demonstrate that HCP-3^{CENP-A} and CPAR-1^{CENP-A}-containing centromeric chromatin and HCP-4^{CENP-C} participate, or are even essential, for the assembly of the outer kinetochore during prometaphase I and II, respectively. Thus, these results underscore the distinct requirements for kinetochore assembly in meiosis I and II. Considering the localization of HCP-3^{CENP-A}, CPAR-1^{CENP-A}, and HCP-4^{CENP-C} throughout meiotic chromosomes, we posit that only the outer layer in direct contact with outer kinetochore components is crucial for cup-like kinetochore assembly during the meiotic divisions.

Our results also clarify previously perplexing findings that suggested the simultaneous dispensability of HCP-3^{CENP-A} and CPAR-1^{CENP-A}, alongside the essentiality of downstream HCP-4^{CENP-C}, for outer kinetochore assembly.[37,51] A plausible cause for the discrepancy between these initial studies and our results lies in the differing methods we employed for depleting CENP-A or CENP-C. The initial studies relied solely on double-stranded RNAs to deplete the two CENP-A paralogs, or CENP-C, via RNAi. By contrast, we used a multifaceted approach: CRISPR-Cas9-based genetic deletion of *cpar-1^{cenp-a}*, RNAi-mediated depletion of *hcp-3^{cenp-a}* or *hcp-4^{cenp-c}* transcripts, coupled to Auxin-induced degradation of the HCP-3^{CENP-A} or HCP-4^{CENP-C} proteins. The combination of methods we employed to deplete CENP-A and CENP-C likely resulted in more effective depletion and consequently stronger phenotypes. Additionally, using an RNAi-mediated depletion approach, CPAR-1^{CENP-A} had previously been considered nonessential in *C. elegans*.[67] Using our *cpar-1^{cenp-a}* full deletion, we show here that it is, in fact, the dominant CENP-A paralog during *C. elegans* meiosis, responsible for the majority of HCP-4^{CENP-C} chromosomal localization. Nonetheless, due to the redundant mechanisms for kinetochore assembly in this model, CPAR-1^{CENP-A} is dispensable for worm viability (Figure S1A).

A unique and fascinating feature of prometaphase I is the co-existence of two parallel pathways for outer kinetochore localization, a centromeric chromatin canonical pathway and a KNL-2^{M18BP1}/MEL-28^{ELYS} non-canonical pathway (Figure 6E).[51] Unlike during mitosis or diakinesis, the localizations of KNL-2^{M18BP1} and the two CENP-A paralogs were not interdependent during prometaphase I. However, KNL-2^{M18BP1} and CENP-A-containing centromeric chromatin coordinately localized MEL-28^{ELYS} at kinetochores, which in turn cooperated with

MEL-28^{ELYS}, KNL-2^{M18BP1}, and indicated outer kinetochore component normalized mean intensities along bivalent chromosomes during prometaphase I. Darker lines represent the mean. Lighter bands represent the SEM. Sample size (*n* homologous chromosome pair) is indicated on the graphs.

(C) Schematic of one homologous chromosome pair (bivalent) and associated cup-like structures. Chromosomes are surrounded by KNL-2^{M18BP1} and MEL-28^{ELYS} internal cups (green). KNL-1^{KNL1}, KNL-3^{DSN1}, BUB-1^{BUB-1}, and KBP-4^{SPC25} formed wider cups (magenta), which surrounded MEL-28^{ELYS} and KNL-2^{M18BP1}. BUB-1^{BUB-1} also localizes at the ring domain located between homologous chromosomes.

See also Figure S6.

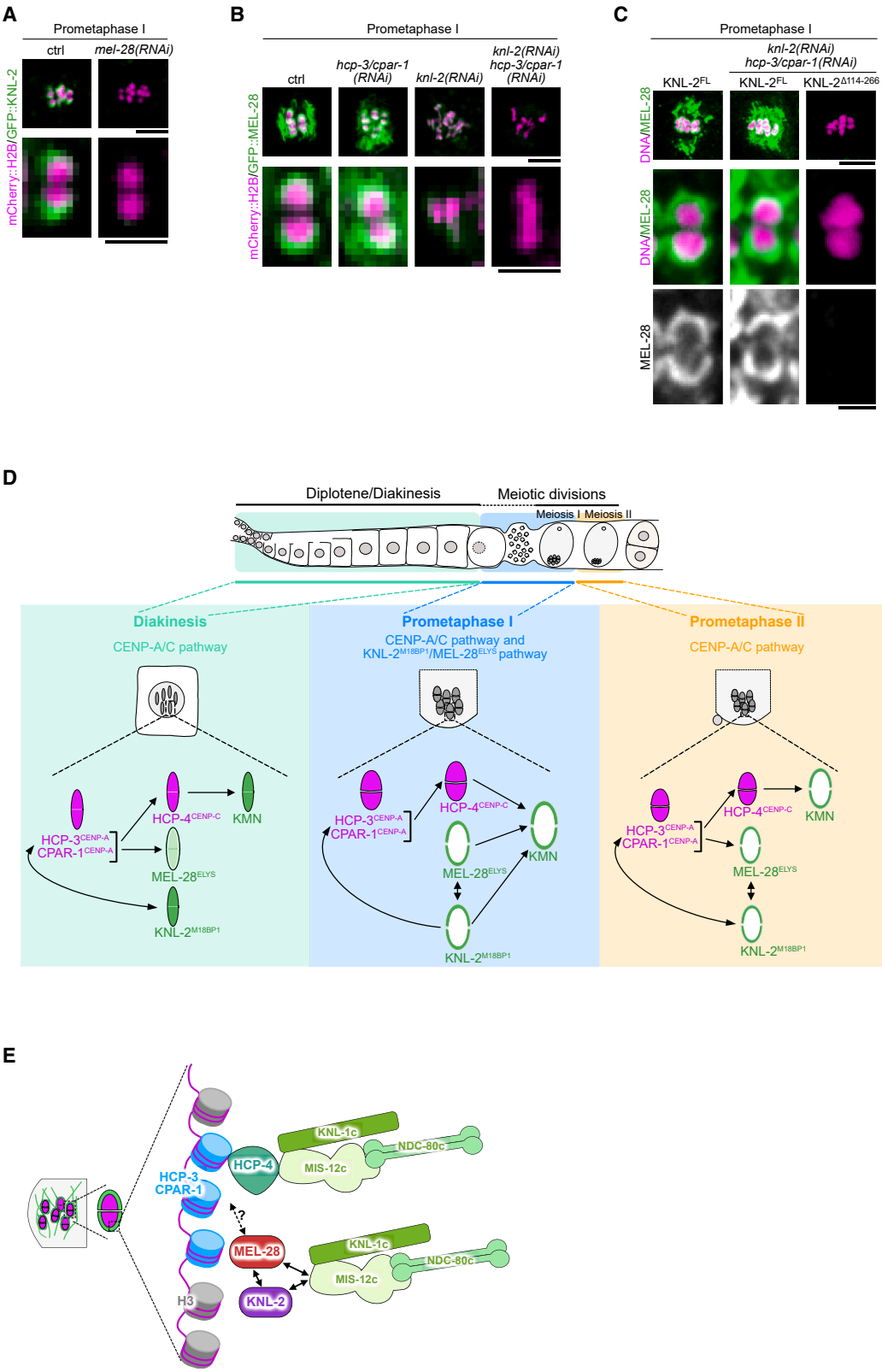

Figure 6. KNL-2^{M18BP1} and MEL-28^{ELYS} are interdependent for their localization at the cup-like kinetochores

(A and B) Representative images of chromosomes in mCherry::HIS-11^{H2B} (magenta) and GFP::KNL-2^{M18BP1} (A) or GFP::MEL-28^{ELYS} (B) (green)-expressing oocytes in indicated conditions. Scale bars, 5 μm. For each condition, bottom: zoom on one homologous chromosome pair; scale bars, 2 μm.

(legend continued on next page)

HCP-4^{CENP-C} for outer kinetochore recruitment. We identified an N-terminal region of KNL-2^{M18BP1} (aa 114–266), predicted to be unfolded and distinct from its three well-defined functional domains, that played a crucial role in this process, although the exact mechanism remains unknown. This region allowed separating the functions of KNL-2^{M18BP1} that ensure proper meiotic chromosome condensation and promote outer kinetochore assembly in oocytes (Figure 4C). In the absence of endogenous KNL-2^{M18BP1}, oocytes expressing the corresponding truncated mutant (Δ114–266) lacked outer kinetochores but displayed properly condensed chromosomes.

A puzzling observation was that, despite supporting normal chromosome condensation, the Δ114–266 KNL-2^{M18BP1} mutant was not localized on chromosomes during prometaphase I. Similarly, in the absence of MEL-28^{ELYS}, KNL-2^{M18BP1} was absent from chromosomes in prometaphase I, yet the chromosomes were visibly well-condensed (Figure 6A). We propose two plausible, and not mutually exclusive, hypotheses to explain these results. First, we found that, unlike during prometaphase I, the chromosomal localization of KNL-2^{M18BP1} during diakinesis depended on CENP-A rather than MEL-28^{ELYS} (Figure S6D). This suggests that the critical function of KNL-2^{ELYS} may occur at this early stage, and its continuous presence on chromosomes may not be necessary for proper chromosome condensation. Second, the essential role of KNL-2^{M18BP1} in promoting proper chromosome condensation could be linked to its presence in the nucleoplasm rather than on chromatin. Indeed, despite not being concentrated on chromosomes, wild-type KNL-2^{M18BP1} in the absence of MEL-28^{ELYS} and the Δ114–266 KNL-2^{M18BP1} mutant should still both be present in the nucleoplasm during diakinesis. This second hypothesis is compatible with our finding that KNL-2^{M18BP1} was delocalized from chromosomes in the absence of HCP-3^{CENP-A} and CPAR-1^{CENP-A}, yet the chromosomes appeared properly condensed (Figure 3C). Determining the precise role of KNL-2^{M18BP1} in the control of meiotic chromosome segregation will require further investigation, and our KNL-2^{M18BP1} separation-of-function mutants should prove useful for this purpose.

What might be the role of the dual mechanism for outer kinetochore assembly that we have identified? In vertebrates, the outer kinetochore is linked to the inner kinetochore via two different pathways. One pathway involves the inner kinetochore scaffold CENP-C, which recruits the outer kinetochore complex Mis12c.[21] The Mis12c complex then recruits the Knl1c and Ndc80c complexes.[68] The second pathway involves the inner kinetochore protein CENP-T, which independently recruits one Mis12c complex and two Ndc80c complexes.[22–25] Although the relative importance of these two pathways varies between species, previous research in chicken and human cells has shown that CENP-T is the dominant pathway in these species.[69–71] By contrast, *C. elegans* lacks a CENP-T ortholog, and during mitosis, HCP-4^{CENP-C} alone appears sufficient for outer kinetochore assembly.[39] We found that depleting MEL-28^{ELYS} alone had no effect on outer kinetochore formation, suggesting that HCP-4^{CENP-C} is also sufficient for assembling the outer kinetochore during oocyte meiosis in *C. elegans* (Figure S6A). However, our results indicate that, unlike in mitosis, an alternative pathway dependent on KNL-2^{M18BP1} and MEL-28^{ELYS} can partially support outer kinetochore formation during prometaphase I when HCP-4^{CENP-C} is absent (Figures 2D, 2F, and S1C). It remains unclear whether this alternative pathway acts merely as a backup mechanism or serves as a functional equivalent to the dominant CENP-T pathway observed in vertebrates. To understand how this alternative pathway functions, it will be crucial to determine if KNL-2^{M18BP1}, MEL-28^{ELYS}, or other unidentified proteins involved in this non-canonical pathway of outer kinetochore assembly physically interact with KMN network components. Future studies should in particular investigate the potential involvement of the other Y-complex nucleoporins in this process.

Overall, how KNL-2^{M18BP1}, MEL-28^{ELYS}, and HCP-4^{CENP-C} activities integrate to promote proper outer kinetochore assembly remains unclear and will require further work. In the holocentric lepidopteran insect *Bombyx mori*, which lacks CENP-A, a protein related to CENP-T is necessary for centromeric chromatin-independent kinetochore assembly.[64,72] Yet it does not fully account for the recruitment of outer kinetochore components.[64] Therefore, it will be intriguing to investigate in future studies whether the non-canonical kinetochore assembly pathway we identified in this study is also operative in *B. mori* and other holocentric species.

RESOURCE AVAILABILITY

Lead contact

Further information and requests for resources and reagents should be directed to and will be fulfilled by the lead contact, Julien Dumont (Julien.dumont@ijm.fr).

Materials availability

All unique and stable resources generated by this study are available from the lead contact without restriction.

Data and code availability

- Accession numbers are listed in the key resources table. The DOI is listed in the key resources table. Microscopy data reported in this paper will be shared by the lead contact upon request.
- This paper does not report original code.
- Any additional information required to reanalyze the data reported in this paper is available from the lead contact upon request.

ACKNOWLEDGMENTS

We thank all members of the Dumont lab for their support and advice. We are grateful to Patricia Moussounda, Téo Bitaille, and Clarisse Picard for providing technical support. We thank Florian Steiner and Dhanya Cheerambathur for the kind gift of *C. elegans* strains used in this study. This work was supported by CNRS and University Paris Cité, by NIH R01GM117407 and R01GM130764 (J.C.C.), by post-doctoral fellowship SPF202004011803 from the Fondation

(C) Top: immunofluorescence images, centered on chromosomes, of oocytes in indicated conditions stained for DNA (magenta) and MEL-28 (green). Scale bar, 5 μm. Bottom: zoom on one homologous chromosome pair; scale bar, 1 μm.
(D) Schematics of the three phases identified for outer kinetochore assembly during oocyte meiosis in *C. elegans*.
(E) Schematics of the model highlighting parallel roles of the centromeric and KNL-2^{M18BP1}/MEL-28^{ELYS}-dependent pathways of outer kinetochore assembly during prometaphase I in *C. elegans* oocytes.

pour la Recherche Médicale (L.B.), and by grants from the European Research Council ERC-CoG ChromoSOMe 819179 and from the Agence Nationale de la Recherche ANR-19-CE13-0015 (J.D.).

AUTHOR CONTRIBUTIONS

L.B. and J.D. conceived the project. L.B. performed most experiments and data analysis with the help of N.M. and L.E.M. N.M. and L.E.M. generated tools and performed essential microscopy experiments. T.G. provided technical support. L.B. and J.D. designed all experiments. L.B., N.M., L.E.M., J.C.C., and J.D. made intellectual contributions. L.B. and J.D. wrote the manuscript. J.C.C. helped with editing. L.B. and J.D. made the figures.

DECLARATION OF INTERESTS

The authors declare no competing interests.

STAR★METHODS

Detailed methods are provided in the online version of this paper and include the following:

- KEY RESOURCES TABLE
- EXPERIMENTAL MODEL AND SUBJECT DETAILS
  - *C. elegans* strain maintenance
  - Transgenesis in *C. elegans*
- METHOD DETAILS
  - RNA-mediated interference
  - Auxin-induced degradation
  - Western blotting
  - Immunofluorescence
  - Microscopy
  - Figure preparation
- QUANTIFICATION AND STATISTICAL ANALYSIS

SUPPLEMENTAL INFORMATION

Supplemental information can be found online at https://doi.org/10.1016/j.cub.2024.09.004.

Received: March 5, 2024
Revised: July 24, 2024
Accepted: September 2, 2024
Published: September 30, 2024

REFERENCES

1. Musacchio, A., and Desai, A. (2017). A molecular view of kinetochore assembly and function. Biology (Basel) *6*, 5. https://doi.org/10.3390/biology6010005.
2. Ariyoshi, M., and Fukagawa, T. (2023). An updated view of the kinetochore architecture. Trends Genet. *39*, 941–953. https://doi.org/10.1016/j.tig.2023.09.003.
3. Cheeseman, I.M., Chappie, J.S., Wilson-Kubalek, E.M., and Desai, A. (2006). The conserved KMN network constitutes the core microtubule-binding site of the kinetochore. Cell *127*, 983–997.
4. Cheeseman, I.M., Niessen, S., Anderson, S., Hyndman, F., Yates, J.R., 3rd, Oegema, K., and Desai, A. (2004). A conserved protein network controls assembly of the outer kinetochore and its ability to sustain tension. Genes Dev. *18*, 2255–2268.
5. Mccleland, M.L., Gardner, R.D., Kallio, M.J., Daum, J.R., Gorbsky, G.J., Burke, D.J., and Stukenberg, P.T. (2003). The highly conserved Ndc80 complex is required for kinetochore assembly, chromosome congression, and spindle checkpoint activity. Genes Dev. *17*, 101–114. https://doi.org/10.1101/gad.1040903.
6. Desai, A., Rybina, S., Müller-Reichert, T., Shevchenko, A., Shevchenko, A., Hyman, A., and Oegema, K. (2003). KNL-1 directs assembly of the microtubule-binding interface of the kinetochore in C. elegans. Genes Dev. *17*, 2421–2435. https://doi.org/10.1101/gad.1126303.
7. Obuse, C., Iwasaki, O., Kiyomitsu, T., Goshima, G., Toyoda, Y., and Yanagida, M. (2004). A conserved Mis12 centromere complex is linked to heterochromatic HP1 and outer kinetochore protein Zwint-1. Nat. Cell Biol. *6*, 1135–1141. https://doi.org/10.1038/ncb1187.
8. Pinsky, B.A., Tatsutani, S.Y., Collins, K.A., and Biggins, S. (2003). An Mtw1 complex promotes kinetochore biorientation that is monitored by the Ipl1/Aurora protein kinase. Dev. Cell *5*, 735–745. https://doi.org/10.1016/s1534-5807(03)00322-8.
9. Yatskevich, S., Yang, J., Bellini, D., Zhang, Z., and Barford, D. (2024). Structure of the human outer kinetochore KMN network complex. Nat. Struct. Mol. Biol. *31*, 874–883. https://doi.org/10.1038/s41594-024-01249-y.
10. Polley, S., Raisch, T., Ghetti, S., Körner, M., Terbeck, M., Gräter, F., Raunser, S., Aponte-Santamaría, C., Vetter, I.R., and Musacchio, A. (2024). Structure of the human KMN complex and implications for regulation of its assembly. Nat. Struct. Mol. Biol. *31*, 861–873. https://doi.org/10.1038/s41594-024-01230-9.
11. Sidhwani, P., and Straight, A.F. (2023). Epigenetic inheritance and boundary maintenance at human centromeres. Curr. Opin. Struct. Biol. *82*, 102694. https://doi.org/10.1016/j.sbi.2023.102694.
12. Stoler, S., Keith, K.C., Curnick, K.E., and Fitzgerald-Hayes, M. (1995). A mutation in CSE4, an essential gene encoding a novel chromatin-associated protein in yeast, causes chromosome nondisjunction and cell cycle arrest at mitosis. Genes Dev. *9*, 573–586.
13. Howman, E.V., Fowler, K.J., Newson, A.J., Redward, S., MacDonald, A.C., Kalitsis, P., and Choo, K.H. (2000). Early disruption of centromeric chromatin organization in centromere protein A (Cenpa) null mice. Proc. Natl. Acad. Sci. USA *97*, 1148–1153.
14. Blower, M.D., and Karpen, G.H. (2001). The role of Drosophila CID in kinetochore formation, cell-cycle progression and heterochromatin interactions. Nat. Cell Biol. *3*, 730–739.
15. Van Hooser, A.A., Ouspenski, I.I., Gregson, H.C., Starr, D.A., Yen, T.J., Goldberg, M.L., Yokomori, K., Earnshaw, W.C., Sullivan, K.F., and Brinkley, B.R. (2001). Specification of kinetochore-forming chromatin by the histone H3 variant CENP-A. J. Cell Sci. *114*, 3529–3542.
16. Buchwitz, B.J., Ahmad, K., Moore, L.L., Roth, M.B., and Henikoff, S. (1999). A histone-H3-like protein in C. elegans. Nature *401*, 547–548.
17. Foltz, D.R., Jansen, L.E.T., Black, B.E., Bailey, A.O., Yates, J.R., and Cleveland, D.W. (2006). The human CENP-A centromeric nucleosome-associated complex. Nat. Cell Biol. *8*, 458–469. https://doi.org/10.1038/ncb1397.
18. Hori, T., Amano, M., Suzuki, A., Backer, C.B., Welburn, J.P., Dong, Y., McEwen, B.F., Shang, W.H., Suzuki, E., Okawa, K., et al. (2008). CCAN makes multiple contacts with centromeric DNA to provide distinct pathways to the outer kinetochore. Cell *135*, 1039–1052. https://doi.org/10.1016/j.cell.2008.10.019.
19. Pesenti, M.E., Raisch, T., Conti, D., Walstein, K., Hoffmann, I., Vogt, D., Prumbaum, D., Vetter, I.R., Raunser, S., and Musacchio, A. (2022). Structure of the human inner kinetochore CCAN complex and its significance for human centromere organization. Mol. Cell *82*, 2113–2131.e8. https://doi.org/10.1016/j.molcel.2022.04.027.
20. Yatskevich, S., Muir, K.W., Bellini, D., Zhang, Z., Yang, J., Tischer, T., Predin, M., Dendooven, T., McLaughlin, S.H., and Barford, D. (2022). Structure of the human inner kinetochore bound to a centromeric CENP-A nucleosome. Science *376*, 844–852. https://doi.org/10.1126/science.abn3810.
21. Screpanti, E., De Antoni, A., Alushin, G.M., Petrovic, A., Melis, T., Nogales, E., and Musacchio, A. (2011). Direct binding of Cenp-C to the Mis12 complex joins the inner and outer kinetochore. Curr. Biol. *21*, 391–398. https://doi.org/10.1016/j.cub.2010.12.039.

22. Rago, F., Gascoigne, K.E., and Cheeseman, I.M. (2015). Distinct organization and regulation of the outer kinetochore KMN network downstream of CENP-C and CENP-T. Curr. Biol. *25*, 671–677. https://doi.org/10.1016/j.cub.2015.01.059.

23. Nishino, T., Rago, F., Hori, T., Tomii, K., Cheeseman, I.M., and Fukagawa, T. (2013). CENP-T provides a structural platform for outer kinetochore assembly. EMBO J. *32*, 424–436. https://doi.org/10.1038/emboj.2012.348.

24. Huis In 't Veld, P.J., Jeganathan, S., Petrovic, A., Singh, P., John, J., Krenn, V., Weissmann, F., Bange, T., and Musacchio, A. (2016). Molecular basis of outer kinetochore assembly on CENP-T. eLife *5*, e21007. https://doi.org/10.7554/eLife.21007.

25. Suzuki, A., Badger, B.L., and Salmon, E.D. (2015). A quantitative description of Ndc80 complex linkage to human kinetochores. Nat. Commun. *6*, 8161. https://doi.org/10.1038/ncomms9161.

26. Groth, A., Corpet, A., Cook, A.J.L., Roche, D., Bartek, J., Lukas, J., and Almouzni, G. (2007). Regulation of replication fork progression through histone supply and demand. Science *318*, 1928–1931. https://doi.org/10.1126/science.1148992.

27. Ramachandran, S., and Henikoff, S. (2015). Replicating nucleosomes. Sci. Adv. *1*, e1500587. https://doi.org/10.1126/sciadv.1500587.

28. Fujita, Y., Hayashi, T., Kiyomitsu, T., Toyoda, Y., Kokubu, A., Obuse, C., and Yanagida, M. (2007). Priming of centromere for CENP-A recruitment by human hMis18alpha, hMis18beta, and M18BP1. Dev. Cell *12*, 17–30.

29. Maddox, P.S., Hyndman, F., Monen, J., Oegema, K., and Desai, A. (2007). Functional genomics identifies a Myb domain-containing protein family required for assembly of CENP-A chromatin. J. Cell Biol. *176*, 757–763.

30. Moree, B., Meyer, C.B., Fuller, C.J., and Straight, A.F. (2011). CENP-C recruits M18BP1 to centromeres to promote CENP-A chromatin assembly. J. Cell Biol. *194*, 855–871. https://doi.org/10.1083/jcb.201106079.

31. Pan, D., Walstein, K., Take, A., Bier, D., Kaiser, N., and Musacchio, A. (2019). Mechanism of centromere recruitment of the CENP-A chaperone HJURP and its implications for centromere licensing. Nat. Commun. *10*, 4046. https://doi.org/10.1038/s41467-019-12019-6.

32. French, B.T., Westhorpe, F.G., Limouse, C., and Straight, A.F. (2017). Xenopus laevis M18BP1 directly binds existing CENP-A nucleosomes to promote centromeric chromatin assembly. Dev. Cell *42*, 190–199.e10. https://doi.org/10.1016/j.devcel.2017.06.021.

33. Carroll, C.W., Milks, K.J., and Straight, A.F. (2010). Dual recognition of CENP-A nucleosomes is required for centromere assembly. J. Cell Biol. *189*, 1143–1155. https://doi.org/10.1083/jcb.201001013.

34. Dunleavy, E.M., Roche, D., Tagami, H., Lacoste, N., Ray-Gallet, D., Nakamura, Y., Daigo, Y., Nakatani, Y., and Almouzni-Pettinotti, G. (2009). HJURP is a cell-cycle-dependent maintenance and deposition factor of CENP-A at centromeres. Cell *137*, 485–497. https://doi.org/10.1016/j.cell.2009.02.040.

35. Foltz, D.R., Jansen, L.E.T., Bailey, A.O., Yates, J.R., 3rd, Bassett, E.A., Wood, S., Black, B.E., and Cleveland, D.W. (2009). Centromere-specific assembly of CENP-a nucleosomes is mediated by HJURP. Cell *137*, 472–484. https://doi.org/10.1016/j.cell.2009.02.039.

36. Maddox, P.S., Oegema, K., Desai, A., and Cheeseman, I.M. (2004). "Holo"er than thou: chromosome segregation and kinetochore function in C. elegans. Chromosome Res. *12*, 641–653.

37. Monen, J., Maddox, P.S., Hyndman, F., Oegema, K., and Desai, A. (2005). Differential role of CENP-A in the segregation of holocentric C. elegans chromosomes during meiosis and mitosis. Nat. Cell Biol. *7*, 1248–1255.

38. Caro, L., Raman, P., Steiner, F.A., Ailion, M., and Malik, H.S. (2022). Recurrent but short-lived duplications of centromeric proteins in holocentric Caenorhabditis species. Mol. Biol. Evol. *39*, msac206. https://doi.org/10.1093/molbev/msac206.

39. Oegema, K., Desai, A., Rybina, S., Kirkham, M., and Hyman, A.A. (2001). Functional analysis of kinetochore assembly in Caenorhabditis elegans. J. Cell Biol. *153*, 1209–1226.

40. de Groot, C., Houston, J., Davis, B., Gerson-Gurwitz, A., Monen, J., Lara-Gonzalez, P., Oegema, K., Shiau, A.K., and Desai, A. (2021). The N-terminal tail of C. elegans CENP-A interacts with KNL-2 and is essential for centromeric chromatin assembly. Mol. Biol. Cell *32*, 1193–1201. https://doi.org/10.1091/mbc.E20-12-0798.

41. Wenda, J.M., Prosée, R.F., Gabus, C., and Steiner, F.A. (2021). Mitotic chromosome condensation requires phosphorylation of the centromeric protein KNL-2 in C. elegans. J. Cell Sci. *134*, jcs259088. https://doi.org/10.1242/jcs.259088.

42. Prosée, R.F., Wenda, J.M., Özdemir, I., Gabus, C., Delaney, K., Schwager, F., Gotta, M., and Steiner, F.A. (2021). Transgenerational inheritance of centromere identity requires the CENP-A N-terminal tail in the C. elegans maternal germ line. PLoS Biol. *19*, e3000968. https://doi.org/10.1371/journal.pbio.3000968.

43. Moore, L.L., and Roth, M.B. (2001). HCP-4, a CENP-C-like protein in Caenorhabditis elegans, is required for resolution of sister centromeres. J. Cell Biol. *153*, 1199–1208.

44. Gassmann, R., Rechtsteiner, A., Yuen, K.W., Muroyama, A., Egelhofer, T., Gaydos, L., Barron, F., Maddox, P., Essex, A., Monen, J., et al. (2012). An inverse relationship to germline transcription defines centromeric chromatin in C. elegans. Nature *484*, 534–537. https://doi.org/10.1038/nature10973.

45. Howe, M., McDonald, K.L., Albertson, D.G., and Meyer, B.J. (2001). HIM-10 is required for kinetochore structure and function on Caenorhabditis elegans holocentric chromosomes. J. Cell Biol. *153*, 1227–1238.

46. Wignall, S.M., and Villeneuve, A.M. (2009). Lateral microtubule bundles promote chromosome alignment during acentrosomal oocyte meiosis. Nat. Cell Biol. *11*, 839–844. https://doi.org/10.1038/ncb1891.

47. Dumont, J., Oegema, K., and Desai, A. (2010). A kinetochore-independent mechanism drives anaphase chromosome separation during acentrosomal meiosis. Nat. Cell Biol. *12*, 894–901. https://doi.org/10.1038/ncb2093.

48. Dumont, J., and Desai, A. (2012). Acentrosomal spindle assembly and chromosome segregation during oocyte meiosis. Trends Cell Biol. *22*, 241–249. https://doi.org/10.1016/j.tcb.2012.02.007.

49. Pereira, C., Reis, R.M., Gama, J.B., Celestino, R., Cheerambathur, D.K., Carvalho, A.X., and Gassmann, R. (2018). Self-assembly of the RZZ complex into filaments drives kinetochore expansion in the absence of microtubule attachment. Curr. Biol. *28*, 3408–3421.e8. https://doi.org/10.1016/j.cub.2018.08.056.

50. Sacristan, C., Ahmad, M.U.D., Keller, J., Fermie, J., Groenewold, V., Tromer, E., Fish, A., Melero, R., Carazo, J.M., Klumperman, J., et al. (2018). Dynamic kinetochore size regulation promotes microtubule capture and chromosome biorientation in mitosis. Nat. Cell Biol. *20*, 800–810. https://doi.org/10.1038/s41556-018-0130-3.

51. Hattersley, N., Schlientz, A.J., Prevo, B., Oegema, K., and Desai, A. (2022). MEL-28/ELYS and CENP-C coordinately control outer kinetochore assembly and meiotic chromosome-microtubule interactions. Curr. Biol. *32*, 2563–2571.e4. https://doi.org/10.1016/j.cub.2022.04.046.

52. Franz, C., Walczak, R., Yavuz, S., Santarella, R., Gentzel, M., Askjaer, P., Galy, V., Hetzer, M., Mattaj, I.W., and Antonin, W. (2007). MEL-28/ELYS is required for the recruitment of nucleoporins to chromatin and postmitotic nuclear pore complex assembly. EMBO Rep. *8*, 165–172. https://doi.org/10.1038/sj.embor.7400889.

53. Galy, V., Askjaer, P., Franz, C., López-Iglesias, C., and Mattaj, I.W. (2006). MEL-28, a novel nuclear-envelope and kinetochore protein essential for zygotic nuclear-envelope assembly in C. elegans. Curr. Biol. *16*, 1748–1756. https://doi.org/10.1016/j.cub.2006.06.067.

54. Gómez-Saldivar, G., Fernandez, A., Hirano, Y., Mauro, M., Lai, A., Ayuso, C., Haraguchi, T., Hiraoka, Y., Piano, F., and Askjaer, P. (2016). Identification of conserved MEL-28/ELYS domains with essential roles in nuclear assembly and chromosome segregation. PLoS Genet. *12*, e1006131. https://doi.org/10.1371/journal.pgen.1006131.

55. Hattersley, N., Cheerambathur, D., Moyle, M., Stefanutti, M., Richardson, A., Lee, K.Y., Dumont, J., Oegema, K., and Desai, A. (2016). A nucleoporin docks protein phosphatase 1 to direct meiotic chromosome segregation and nuclear assembly. Dev. Cell *38*, 463–477. https://doi.org/10.1016/j.devcel.2016.08.006.

56. Yamamoto, I., Kosinski, M.E., and Greenstein, D. (2006). Start me up: cell signaling and the journey from oocyte to embryo inC. elegans. Dev. Dyn. *235*, 571–585. https://doi.org/10.1002/(ISSN)1097-0177.

57. Petrovic, A., Keller, J., Liu, Y., Overlack, K., John, J., Dimitrova, Y.N., Jenni, S., van Gerwen, S., Stege, P., Wohlgemuth, S., et al. (2016). Structure of the MIS12 complex and molecular basis of its interaction with CENP-C at human kinetochores. Cell *167*, 1028–1040.e15. https://doi.org/10.1016/j.cell.2016.10.005.

58. Macaisne, N., Bellutti, L., Laband, K., Edwards, F., Pitayu-Nugroho, L., Gervais, A., Ganeswaran, T., Geoffroy, H., Maton, G., Canman, J.C., et al. (2023). Synergistic stabilization of microtubules by BUB-1, HCP-1, and CLS-2 controls microtubule pausing and meiotic spindle assembly. eLife *12*, e82579. https://doi.org/10.7554/eLife.82579.

59. Cheerambathur, D.K., Prevo, B., Chow, T.L., Hattersley, N., Wang, S., Zhao, Z., Kim, T., Gerson-Gurwitz, A., Oegema, K., Green, R., et al. (2019). The kinetochore-microtubule coupling machinery is repurposed in sensory nervous system morphogenesis. Dev. Cell *48*, 864–872.e7. https://doi.org/10.1016/j.devcel.2019.02.002.

60. Danlasky, B.M., Panzica, M.T., McNally, K.P., Vargas, E., Bailey, C., Li, W., Gong, T., Fishman, E.S., Jiang, X., and McNally, F.J. (2020). Evidence for anaphase pulling forces during C. elegans meiosis. J. Cell Biol. *219*, e202005179. https://doi.org/10.1083/jcb.202005179.

61. A.M. Pitayu-Nugroho, L., Laband, K., Geoffroy, H., Ganeswaran, T., Primadhanty, A., Canman, J.C., and Dumont, J. (2023). Differential requirement for kinetochore components between meiosis and mitosis revealed by 4D tracking of holocentric chromosomes in C. elegans oocytes. Nat. Commun.

62. Okada, M., Cheeseman, I.M., Hori, T., Okawa, K., Mcleod, I.X., Yates, J.R., Desai, A., and Fukagawa, T. (2006). The CENP-H-I complex is required for the efficient incorporation of newly synthesized CENP-A into centromeres. Nat. Cell Biol. *8*, 446–457. https://doi.org/10.1038/ncb1396.

63. Amano, M., Suzuki, A., Hori, T., Backer, C., Okawa, K., Cheeseman, I.M., and Fukagawa, T. (2009). The CENP-S complex is essential for the stable assembly of outer kinetochore structure. J. Cell Biol. *186*, 173–182. https://doi.org/10.1083/jcb.200903100.

64. Cortes-Silva, N., Ulmer, J., Kiuchi, T., Hsieh, E., Cornilleau, G., Ladid, I., Dingli, F., Loew, D., Katsuma, S., and Drinnenberg, I.A. (2020). CenH3-independent kinetochore assembly in Lepidoptera requires CCAN, including CENP-T. Curr. Biol. *30*, 561–572.e10. https://doi.org/10.1016/j.cub.2019.12.014.

65. Zhang, D., Martyniuk, C.J., and Trudeau, V.L. (2006). SANTA domain: a novel conserved protein module in Eukaryota with potential involvement in chromatin regulation. Bioinformatics *22*, 2459–2462. https://doi.org/10.1093/bioinformatics/btl414.

66. Ohzeki, J., Bergmann, J.H., Kouprina, N., Noskov, V.N., Nakano, M., Kimura, H., Earnshaw, W.C., Larionov, V., and Masumoto, H. (2012). Breaking the HAC Barrier: histone H3K9 acetyl/methyl balance regulates CENP-A assembly. EMBO J. *31*, 2391–2402. https://doi.org/10.1038/emboj.2012.82.

67. Monen, J., Hattersley, N., Muroyama, A., Stevens, D., Oegema, K., and Desai, A. (2015). Separase cleaves the N-tail of the CENP-A related protein CPAR-1 at the meiosis I metaphase-anaphase transition in C. elegans. PLoS One *10*, e0125382. https://doi.org/10.1371/journal.pone.0125382.

68. Petrovic, A., Pasqualato, S., Dube, P., Krenn, V., Santaguida, S., Cittaro, D., Monzani, S., Massimiliano, L., Keller, J., Tarricone, A., et al. (2010). The MIS12 complex is a protein interaction hub for outer kinetochore assembly. J. Cell Biol. *190*, 835–852. https://doi.org/10.1083/jcb.201002070.

69. Hara, M., Ariyoshi, M., Sano, T., Nozawa, R.S., Shinkai, S., Onami, S., Jansen, I., Hirota, T., and Fukagawa, T. (2023). Centromere/kinetochore is assembled through CENP-C oligomerization. Mol. Cell *83*, 2188–2205.e13. https://doi.org/10.1016/j.molcel.2023.05.023.

70. Takenoshita, Y., Hara, M., and Fukagawa, T. (2022). Recruitment of two Ndc80 complexes via the CENP-T pathway is sufficient for kinetochore functions. Nat. Commun. *13*, 851. https://doi.org/10.1038/s41467-022-28403-8.

71. Sissoko, G.B., Tarasovetc, E.V., Marescal, O., Grishchuk, E.L., and Cheeseman, I.M. (2024). Higher-order protein assembly controls kinetochore formation. Nat. Cell Biol. *26*, 45–56. https://doi.org/10.1038/s41556-023-01313-7.

72. Drinnenberg, I.A., deYoung, D., Henikoff, S., and Malik, H.S. (2014). Recurrent loss of CenH3 is associated with independent transitions to holocentricity in insects. eLife *3*, e03676. https://doi.org/10.7554/eLife.03676.

73. Schindelin, J., Arganda-Carreras, I., Frise, E., Kaynig, V., Longair, M., Pietzsch, T., Preibisch, S., Rueden, C., Saalfeld, S., Schmid, B., et al. (2012). Fiji: an open-source platform for biological-image analysis. Nat. Methods *9*, 676–682. https://doi.org/10.1038/nmeth.2019.

74. Brenner, S. (1974). The genetics of Caenorhabditis elegans. Genetics *77*, 71–94.

75. Frøkjaer-Jensen, C., Davis, M.W., Hopkins, C.E., Newman, B.J., Thummel, J.M., Olesen, S.-P., Grunnet, M., and Jorgensen, E.M. (2008). Single-copy insertion of transgenes in Caenorhabditis elegans. Nat. Genet. *40*, 1375–1383. https://doi.org/10.1038/ng.248.

76. Laband, K., Lacroix, B., Edwards, F., Canman, J.C., and Dumont, J. (2018). Live imaging of C. elegans oocytes and early embryos. Methods Cell Biol. *145*, 217–236. https://doi.org/10.1016/bs.mcb.2018.03.025.

77. Sievers, F., Wilm, A., Dineen, D., Gibson, T.J., Karplus, K., Li, W., Lopez, R., McWilliam, H., Remmert, M., Söding, J., et al. (2011). Fast, scalable generation of high-quality protein multiple sequence alignments using Clustal Omega. Mol. Syst. Biol. *7*, 539. https://doi.org/10.1038/msb.2011.75.

78. Waterhouse, A.M., Procter, J.B., Martin, D.M., Clamp, M., and Barton, G.J. (2009). Jalview Version 2--a multiple sequence alignment editor and analysis workbench. Bioinformatics *25*, 1189–1191. https://doi.org/10.1093/bioinformatics/btp033.

STAR★METHODS

KEY RESOURCES TABLE

REAGENT or RESOURCE	SOURCE	IDENTIFIER
Antibodies		
Mouse monoclonal anti-GFP	Roche	RRID: AB_390913
Rabbit anti-GFP	Custom-produced	N/A
Mouse monoclonal anti-HA tag	Institut Curie, Paris, FR	N/A
Rabbit anti-MEL-28	Galy et al.[53]	N/A
Mouse anti-αtubulin DM1α	Abcam	RRID: AB_2241126
Mouse anti-βactin (C4)	Santa Cruz Biotechnology	RRID: AB_2714189
Donkey anti-Mouse IgG (H+L) Cross-Absorbed Secondary Antibody, DyLight 650	Thermo Scientific	RRID: AB_2556749
Donkey anti-Mouse IgG (H+L) Highly Cross-Adsorbed Secondary Antibody, Alexa Fluor 488	Thermo Scientific	RRID: AB_141607
Donkey anti-Mouse IgG (H+L) Highly Cross-Adsorbed Secondary Antibody, Alexa Fluor 594	Thermo Scientific	RRID: AB_141633
Rabbit polyclonal anti-KNL-1	Desai et al.[6]	N/A
Rabbit polyclonal anti-KNL-2	Maddox et al.[29]	N/A
Rabbit polyclonal anti-KNL-3	Cheeseman et al.[4]	N/A
Rabbit polyclonal anti-HCP-4	Oegema et al.[39]	N/A
Rabbit polyclonal anti-BUB-1	Oegema et al.[39]	N/A
Rabbit polyclonal anti-KBP-4	Cheeseman et al.[4]	N/A
Bacterial and virus strains		
E. coli Strain: OP50-1	Caenorhabditis Genetics Center (CGC)	N/A
Chemicals, peptides, and recombinant proteins		
Indole-3-acetic acid sodium salt	Sigma-Aldrich	Cat # I5148
MEGAscript T3 Transcription Kit	Invitrogen	Cat#AM1338
MEGAscript T7 Transcription Kit	Invitrogen	Cat#AM1334
MEGAclear	Invitrogen	Cat#AM1908
Experimental models: Organisms/strains		
C. elegans: Strain wild type N2 (ancestral)	Caenorhabditis Genetics Center (CGC)	N2
C. elegans: Strain FAS155: *uge70*[*knl-2*::HA]I; *uge105*[OLLAS::AID::*hcp-3*]III; *ieSi38*[*sun-1p*::TIR1::mRuby::*sun-1* 3'UTR + *Cb-unc-119(+)*]IV	Prosée et al.[42]	FAS155
C. elegans: Strain FAS163: *uge85*[GFP::HA::*hcp-3*])III; *uge110*[*knl-2*::OLLAS::AID])I; *ieSi38*[*sun-1p*::TIR1::mRuby::*sun-1* 3'UTR + *Cb-unc-119(+)*]IV	Prosée et al.[42]	FAS163
C. elegans: Strain PHX4525: *syb4525* [OLLAS::AID::*hcp-4*]) I	This study, produced by Suny Biotech	PHX4525
C. elegans: Strain JDU606: *lt78*[GFP::*hcp-3*]I; *ijmSi31*[*mex-5p*::mCherry::*his-11*::*tbb-2* 3'UTR]II; *unc-119(ed3)*III?	This study	JDU606
C. elegans: Strain JDU624: *cenp-x(ijm17)*IV	This study	JDU624
C. elegans: Strain JDU628: *ijmSi133*[*mex-5p*::GFP::*cenp-x*::*tbb-2* 3'UTR + mCherry::*his-11*::*tbb-2* 3'UTR + *Cb-unc-119(+)*]I; *unc-119(ed3)*III	This study	JDU628

(*Continued on next page*)

Continued

REAGENT or RESOURCE	SOURCE	IDENTIFIER
C. elegans: Strain JDU641: *cenp-s(ijm18)*III	This study	JDU641
C. elegans: Strain JDU643: *ijmSi132*[*mex-5p*::GFP::*cenp-s*::*tbb-2* 3'UTR + mCherry::*his-11*::*tbb-2* 3'UTR + *Cb-unc-119(+)*]I; *unc-119(ed3)*III	This study	JDU643
C. elegans: Strain JDU664: *ijmSi31*[*mex-5p*::mCherry::*his-11*::*tbb-2* 3'UTR]II; *bq5*[GFP::*mel-28*]III, *unc-119(ed3)*III?	This study	JDU664
C. elegans: Strain JDU670: *uge105*[OLLAS::AID::*hcp-3*]III; *ieSi38*[*sun-1p*::TIR1::mRuby::*sun-1* 3'UTR + *Cb-unc-119(+)*]IV; *F20D6.9(ijm23)*V	This study	JDU670
C. elegans: Strain JDU681: *uge70*[*knl-2*::HA]I; *cpar-1(ijm26)*III, *uge105*[OLLAS::AID::*hcp-3*]III; *ieSi38*[*sun-1p*::TIR1::mRuby::*sun-1* 3'UTR + *Cb-unc-119(+)*]IV	This study	JDU681
C. elegans: Strain JDU682: *cpar-1(ijm26)*III, *uge105*[OLLAS::AID::*hcp-3*]III; *ieSi38*[*sun-1p*::TIR1::mRuby::*sun-1* 3'UTR + *Cb-unc-119(+)*]IV; *F20D6.9(ijm23)*V	This study	JDU682
C. elegans: Strain JDU698: *syb4525*[OLLAS::AID::*hcp-4*]I; *ieSi38*[*sun-1p*::TIR1::mRuby::*sun-1* 3'UTR + *Cb-unc-119(+)*]IV	This study	JDU698
C. elegans: Strain JDU708 ijmSi139[Pmex-5::GFP::F20D6.9 + mCherry-his11 + Cbr-unc-119(+)]I; unc-119(ed3)III	This study	JDU708
C. elegans: Strain JDU709 syb4525[OLLAS::Degron::hcp-4]I; ijmSi31[Pmex-5::mCherry::his-11::tbb-2 3'UTR]II; unc-119(ed3)III?; ieSi38[sun-1p::TIR1::mRuby::sun-1 3'UTR + Cbr-unc-119(+)]IV; lt46[GFP::knl-3])V	This study	JDU709
C. elegans: Strain JDU710 syb4525[OLLAS::Degron::hcp-4]I; ijmSi31[Pmex-5::mCherry::his-11::tbb-2 3'UTR]II, knl-1(lt53[knl-1::GFP::tev::loxP::3xFlag]))III, unc-119(ed3) III?, ieSi38 [sun-1p::TIR1::mRuby::sun-1 3'UTR + Cbr-unc-119(+)]IV	This study	JDU710
C. elegans: Strain JDU733 ijmSi31[Pmex-5::mCherry::his-11::tbb-2 3'UTR]II; ijm36 (cpar-1::GFP)III; unc-119(ed3)III?	This study	JDU733
C. elegans: Strain JDU738 lt73[GFP::knl-2]I; ijmSi31[Pmex-5::mCherry::his-11::tbb-2 3'UTR]II; unc-119(ed3)III?	This study	JDU738
C. elegans: Strain JDU759 ijmSi31[Pmex-5::mCherry::his-11::tbb-2 3'UTR]II; cpar-1 (ijm26)III, uge105[OLLAS::Degron::hcp-3])III, unc-119(ed3)III?; ieSi38[sun-1p::TIR1::mRuby::sun-1 3'UTR + Cbr-unc-119(+)]IV; lt46[GFP::knl-3]V	This study	JDU759
C. elegans: Strain JDU794 uge110[knl-2::OLLAS::Degron]I; ijmSi157[knl-2_reencoded_Δaa114-622::GFP + Cbr-unc-119(+)]II; it75 [knl-1::mCherry]III; ieSi38[sun-1p::TIR1::mRuby::sun-1 3'UTR + Cbr-unc-119(+)]IV	This study	JDU794
C. elegans: Strain JDU795 uge110[knl-2::OLLAS::Degron]I; ijmSi156[knl-2_reencoded_Δaa2-113::GFP + Cbr-unc-119(+)]II; it75[knl-1::mCherry]III; ieSi38[sun-1p::TIR1::mRuby::sun-1 3'UTR + Cbr-unc-119(+)]IV	This study	JDU795

(*Continued on next page*)

Continued

REAGENT or RESOURCE	SOURCE	IDENTIFIER
C. elegans: Strain JDU796 uge110[knl-2::OLLAS::Degron])I; ijmSi158[knl-2_reencoded_Δaa623-877::GFP + Cbr-unc-119(+)]II; it75 [knl-1::mCherry]III; ieSi38[sun-1p::TIR1::mRuby::sun-1 3'UTR + Cbr-unc-119(+)]IV	This study	JDU796
C. elegans: Strain JDU797 uge110[knl-2::OLLAS::Degron]I;ijmSi152[knl-2_reencoded_Δaa267-470::GFP; Cbr-unc-119(+)]II;it75 [knl-1::mCherry]III;ieSi38[sun-1p::TIR1::mRuby::sun-1 3'UTR + Cbr-unc-119(+)]IV	This study	JDU797
C. elegans: Strain JDU798 uge110[knl-2::OLLAS::Degron]I; ijmSi154[knl2_reencoded::GFP + Cbr-unc-119(+)]II; it75[knl-1::mCherry]III; ieSi38[sun-1p::TIR1::mRuby::sun-1 3'UTR + Cbr-unc-119(+)]IV	This study	JDU798
C. elegans: Strain JDU814 lt73[GFP::knl-2]I; ijmSi31[Pmex-5::mCherry::his-11::tbb-2 3'UTR]II; uge105[OLLAS::Degron::hcp-3]III, unc-119(ed3)III?; ieSi38[sun-1p::TIR1::mRuby::sun-1 3'UTR + Cbr-unc-119(+)]IV	This study	JDU814
C. elegans: Strain JDU816 lt73[GFP::knl-2]I; ijmSi31[Pmex-5::mCherry::his-11::tbb-2 3'UTR]II; cpar-1 (ijm26)III, uge105[OLLAS::Degron::hcp-3]III, unc-119(ed3)III?; ieSi38 [sun-1p::TIR1::mRuby::sun-1 3'UTR + Cbr-unc-119(+)]IV	This study	JDU816
C. elegans: Strain JDU824 uge110[knl-2::OLLAS::Degron]I;ijmSi152[knl-2_reencoded_Δaa114-266::GFP; Cbr-unc-119(+)]II;it75 [knl-1::mCherry]III;ieSi38[sun-1p::TIR1::mRuby::sun-1 3'UTR + Cbr-unc-119(+)]IV	This study	JDU824
C. elegans: Strain JDU825 uge110[knl-2::OLLAS::Degron]I;ijmSi152[knl-2_reencoded_Δaa471-622::GFP; Cbr-unc-119(+)]II;it75[knl-1::mCherry]III;ieSi38[sun-1p::TIR1::mRuby::sun-1 3'UTR + Cbr-unc-119(+)]IV	This study	JDU825
Oligonucleotides		
Primer 1 for synthesis of dsRNA targeting *hcp-3 and cpar-1* AATTAACCCTCACTAA AGGgccgatgacaccccaattat	N/A	N/A
Primer 2 for synthesis of dsRNA targeting *hcp-3 and cpar-1* TAATACGACTCACTAT AGGgttccttccggctctcatc	N/A	N/A
Primer 1 for synthesis of dsRNA targeting *hcp-4* AATTAACCCTCACTAAAGGgggaaa tgtacggagcgaaaa	N/A	N/A
Primer 2 for synthesis of dsRNA targeting *hcp-4* TAATACGACTCACTATAGGacattg ttggtgggtccaat	N/A	N/A
Primer 1 for synthesis of dsRNA targeting *knl-2* AATTAACCCTCACTAAAGGtcgactt ggtcggacagatt	N/A	N/A
Primer 2 for synthesis of dsRNA targeting *knl-2* TAATACGACTCACTATAGGtgcgata tgtggcgttatgt	N/A	N/A

(*Continued on next page*)

Continued

REAGENT or RESOURCE	SOURCE	IDENTIFIER
Primer 1 for synthesis of dsRNA targeting *mel-28* AATTAACCCTCACTAAAGGcgtca gcggttcagttcttc	N/A	N/A
Primer 2 for synthesis of dsRNA targeting *mel-28* TAATACGACTCACTATAGGcgtgt cctggatgttctgg	N/A	N/A
sgRNA 1 for F35H10.5 deletion AGTAAGATCGATGTTGATTG	N/A	N/A
sgRNA 2 for F35H10.5 deletion ATCGAGACTGACCAATACTG	N/A	N/A
sgRNA 1 for Y48E1C.1 deletion ACAGATAATGGGAGACCCTG	N/A	N/A
sgRNA 2 for Y48E1C.1 deletion CTTGGAGCAGCACGGAGCAT	N/A	N/A
sgRNA 1 for CPAR-1 deletion GATTTGGAAGGCAAAGACGG	N/A	N/A
sgRNA 2 for CPAR-1 deletion CTTCGAACAATGGCCGATGA	N/A	N/A
sgRNA 1 for F20D6.9 deletion CTCTTCTGTTGGGTTCGGTG	N/A	N/A
sgRNA 2 for F20D6.9 deletion CGTAGCTTCGAAGTCAACTG	N/A	N/A
Recombinant DNA		
pjW68-pCFJ151_knl2_reencoded_GFP	This study	pJD914
pJD914_pjW68-pCFJ151_knl-2_ reenc_ Δaa2-113_GFP	This study	pJD933
pJD914_pjW68-pCFJ151_knl-2_ reenc_Δaa114-622_GFP	This study	pJD934
pJD914_pjW68-pCFJ151_knl-2_ reenc_Δaa623-877_GFP	This study	pJD935
pJD914_pjW68-pCFJ151_knl-2_ reencoded_Δaa114-266_GFP	This study	pJD964
pJD914_pjW68-pCFJ151_knl-2_ reencoded_Δaa471-622_GFP	This study	pJD965
Software and algorithms		
Fiji	Schindelin et al.[73]	RRID: SCR_002285
Prism	GraphPad	RRID: SCR_002798
Designer	Affinity	RRID: SCR_016952
Adobe Illustrator	Adobe	RRID: SCR_010279
Jalview	https://www.jalview.org/	RRID:SCR_006459
Clustal Omega	https://www.ebi.ac.uk/jdispatcher/msa/clustalo	RRID: SCR_001591
SnapGene	Dotmatics	RRID: SCR_015052

EXPERIMENTAL MODEL AND SUBJECT DETAILS

C. elegans strain maintenance

C. elegans strains used in this study were maintained at 20°C or 23°C on nematode growth medium (51 mM NaCl, 2,5 g Bacto Peptone, 17 g Bacto Agar, 12 μM cholesterol, 1 mM $CaCl_2$, 1 mM $MgSO_4$, 25 μM KH_2PO_4 and 5 μM Nystatin in a 1 L ddH2O final) plates and fed with OP50 *E. coli*.[74]

Transgenesis in *C. elegans*

All strains were generated by CRISPR/Cas9-mediated mutagenesis, by Mos1-mediated Single Copy Insertion (MoSCI)[75] or by crossing pre-existing strains. The strains used in this study are listed in the key resources table. All strains produced will be provided upon request and/or made available through the *Caenorhabditis* Genetics Center (CGC, https://cgc.umn.edu/).

METHOD DETAILS

RNA-mediated interference

DNA was amplified by PCR from N2 gDNA or cDNA prepared for total worm extracts. Primers used for amplification are listed below. PCR reactions were cleaned (QIAquick Gel Extraction Kit, Qiagen #28704) and used as templates for T3 and T7 transcription reactions (MEGAscript transcription kit, Invitrogen #AM1334 for T7 and #AM1338 for T3) for 5 hours at 37°C. In vitro transcribed RNAs were purified (MEGAclear kit, Invitrogen), then annealed at 68°C for 10 minutes, followed by 37°C for 30 min. Aliquots were snap frozen in liquid nitrogen and stored at -80°C. L4-stage hermaphrodite larvae were micro-injected with 1500–2000 μg/μL of each dsRNA, and recovered at 20°C for 48 hours before being further processed.

The ds-RNAs used in this study targeted the following genes:
hcp-3 and *cpar-1:* 5'-AATTAACCCTCACTAAAGGgccgatgacaccccaattat-3'
5'-TAATACGACTCACTATAGGgttccttccggctctcatc-3'
hcp-4: 5'-AATTAACCCTCACTAAAGGggaaatgtacggagcgaaaa-3'
5'-TAATACGACTCACTATAGGacattgttggtgggtccaat-3'
knl-2: 5'-AATTAACCCTCACTAAAGGtcgacttggtcggacagatt-3'
5'-TAATACGACTCACTATAGGtgcgatatgtggcgttatgt-3'
mel-28: 5'-AATTAACCCTCACTAAAGGcgtcagcggttcagttcttc-3'
5'-TAATACGACTCACTATAGGcgtgtcctggatgttctgg-3'

Auxin-induced degradation

To implement the auxin-induced degradation system, *C. elegans* strains with *hcp-3, hcp-4* or *knl-2* endogenously tagged with an auxin-inducible degron (mAID) were obtained or generated. The TIR1 transgene used (sun-1p::TIR1::mRuby::sun-1 3'UTR) is under the control of the germline specific sun-1 promoter. We crossed *hcp-3* and *hcp-4* mAID-fused strains with a strain expressing mCherry::HIS-11^{H2B}, under the control of the germline specific *mex-5* promoter, and KNL-3 endogenously tagged with GFP (it46[GFP::knl-3]). We crossed the knl-2 mAID-fused strain with strains expressing KNL-2::GFP transgenes, or KNL-1 endogenously-tagged with mCherry (it75[knl-1::mCherry]).

For auxin depletions, we used NGM plates supplemented with 4 mM auxin seeded with OP50 bacteria. Adult worms were plated overnight before performing live imaging.

Western blotting

For each sample, 100 gravid adult worms (24 hours post-L4) were washed in M9 buffer (22 mM KH_2PO_4, 42 mM Na_2HPO_4, 86 mM NaCl, and 1 mM $MgSO_4 \cdot 7H_2O$) supplemented with 0.1% Triton X100. Samples were then resuspended in 15 μL Laemmli buffer (1X final) and incubated at 97°C for 10 minutes. Worm extracts were loaded on 8% gel. Proteins were then transferred at 90 Volts for 80 minutes in Towbin buffer with SDS at 4°C onto nitrocellulose membranes, which were incubated with 1 μg/mL primary antibodies in 1X TBS-Tween (TBS-T) supplemented with 5% skim milk. A custom-produced Rabbit Anti-GFP antibody was used to specifically detect the transgenes. A mouse anti-ßactin antibody (Santa Cruz Biotechnology Cat# sc-47778) was used as a loading control. Blocking was performed in 1X TBS-Tween supplemented with 5% skim milk, and washes in 1X TBS-T. Signals were sequentially revealed with HRP-coupled goat anti-rabbit and anti-mouse secondary antibodies (Jackson ImmunoResearch 115-035-003 or 11-035-003, 1:10000 in 5% skim milk TBS-T) incubated 1 hour at room temperature. Imaging was performed on a Biorad ChemiDoc Imaging System.

Immunofluorescence

Fifteen to twenty adult worms were dissected in a 3.5 μL droplet of meiosis medium on a glass slide coated with subbing solution (100 mL Milli-Q H_2O, 0.4 g Gelatin USP (Sigma, G1890), 0.04 g Chromalum (Sigma, 243361), 100 mg Poly-L- Lysine (Sigma, P-1524)). Worms were cut to release embryos, oocytes and gonads. A 12x12 mm #1 coverslip (Marienfeld, 0101000) was gently placed on the sample and slides were carefully immersed in liquid nitrogen. After freeze crack, fixation was performed in cold (–20°C) methanol for 15 minutes. Samples were rehydrated twice in 1X PBS for 5 minutes, and blocked 30 minutes at room temperature in AbDil (PBS plus 2% BSA, 0.1% Triton X-100) in a humidified chamber. Unlabeled primary antibodies were diluted at 1 μg/mL in AbDil, and incubated 2 hours at room temperature. Samples were washed twice with AbDil, followed by 1 hour incubation with fluorescently-labeled secondary antibodies at room temperature. Alternatively, fluorescently-labeled primary antibodies diluted in AbDil were incubated 1 hour at room temperature. After two washes with AbDil, DNA was counterstained with 2 μg/mL Hoechst 33342 for 10 minutes at room temperature. After 2 washes with PBS, 0.1%Triton X-100 and one with 1X PBS, samples were mounted in a droplet of mounting medium (0.5% phenylenediamine in 90% glycerol, 20 mM Tris pH 8.8) between the coated glass slide and an 18x18 mm #1.5 glass coverslips (Marienfeld, 0102032). Glass coverslips were sealed with nail polish and stored at -20°C until acquisition.

All antibodies used for immunofluorescence in this study are listed in the key resources table. Z-sections were acquired every 0.2 μm using a Nikon APO λS 100 x/1.45 oil objective. A single Z-plan or maximum projections of relevant sections are presented.

Microscopy

All live and fixed acquisitions were performed using a Nikon Ti-E inverted microscope, equipped with a Yokogawa CSU-X1 spinning-disk confocal head with an emission filter wheel (Yokogawa), a laser launch with a 110 mW-405 nm, a 150 mW-488 nm, a 100 mW-561 nm, and a 110 mW-642 nm laser (Gataca Systems) using a CoolSNAP HQ2 CCD camera (Photometrics). The laser power was measured before each experiment with an Ophir VEGA Laser and energy meter. Fine stage control and focus correction during acquisition was performed with a PZ-2000 XYZ Piezo-driven motor from Applied Scientific Instrumentation. The microscope was controlled with Metamorph 7 software (Molecular Devices). Image analysis was performed using the Fiji software.[73]

For *ex utero* live imaging of *C. elegans* fertilized oocytes, adult worms were dissected on a coverslip in 4 μL meiosis medium (5 mg/mL inulin, 25 mM HEPES, 60% Leibovitz's L-15 media and 20% fetal bovine).[76] Movies were acquired using a Nikon CFI APO S 60x/NA1.4 oil immersion objective with 2x2 binning. For all movies, 4 Z-plans, separated by 2 μm, were acquired every 15 seconds. Temperature during imaging was maintained constant at 23°C using the CherryTemp temperature controller system (CherryBiotech).

Embryonic viability assays

Embryonic viability assays were performed at 20°C. Worms were singled onto plates 36 hours post-L4. Worms were allowed to lay eggs for 16 hours before being removed from the laying plates. Plates were then left at 20°C for another 36 hours before the total number of unhatched eggs and of worms was counted. The proportion of viable progenies was calculated as the number of worms divided by the number of unhatched eggs.

In silico *protein sequence analyses*

Protein sequence alignments were performed using Clustal Omega[77] and visualized with the Jalview software.[78]

Figure preparation

Figures and illustrations were done in the Affinity Designer software (ver. 2.5.3).

QUANTIFICATION AND STATISTICAL ANALYSIS

Fluorescence intensity of KNL-3 at kinetochores and of DNA (Hoechst) (Figures 2, 3, and S6) was measured on projections of 4 Z-planes using line scans along the long axis of prometaphase I chromosomes. Background noise for KNL-3 signal was measured using a line scan of similar length and width outside the chromosome area. Values of the background line scan were averaged, and normalization was performed by subtracting and dividing KNL-3 fluorescence values by the mean background intensity. Then, for each cup-like structure, the three max values immediately outside the DNA area, which thus correspond to the cup-like kinetochores, along the normalized line scan were averaged and plotted.

For Figure 3A, DNA, KNL-2^{M18BP1}, MEL-28^{ELYS} and KNL-1^{KNL-1} intensities along the long axis of prometaphase I chromosomes were measured on a single focal plane using line scans centered at the mid-bivalent. Intensity measurements were normalized to the max intensity value.

For Figure 2E, *ex-utero* live imaging oocyte movies were analyzed to visually score segregation defects at meiosis I and meiosis II. Graphs represent the percentage of oocytes showing normal segregating chromosomes, mis segregating chromosomes or non-segregating chromosomes. "Mis segregation" include lagging or co-segregating chromosomes; "non segregation" refers to chromosome spreading in different directions, without displaying a clear axis of segregation.

GraphPad Prism 10 was used to generate Graphical representation of data and statistical analysis. Statistical tests used are specified in the corresponding figure legends.

Current Biology, Volume *34*

Supplemental Information

Regulation of outer kinetochore assembly during meiosis I and II by CENP-A and KNL-2/M18BP1 in *C. elegans* oocytes

Laura Bellutti, Nicolas Macaisne, Layla El Mossadeq, Thadshagine Ganeswaran, Julie C. Canman, and Julien Dumont

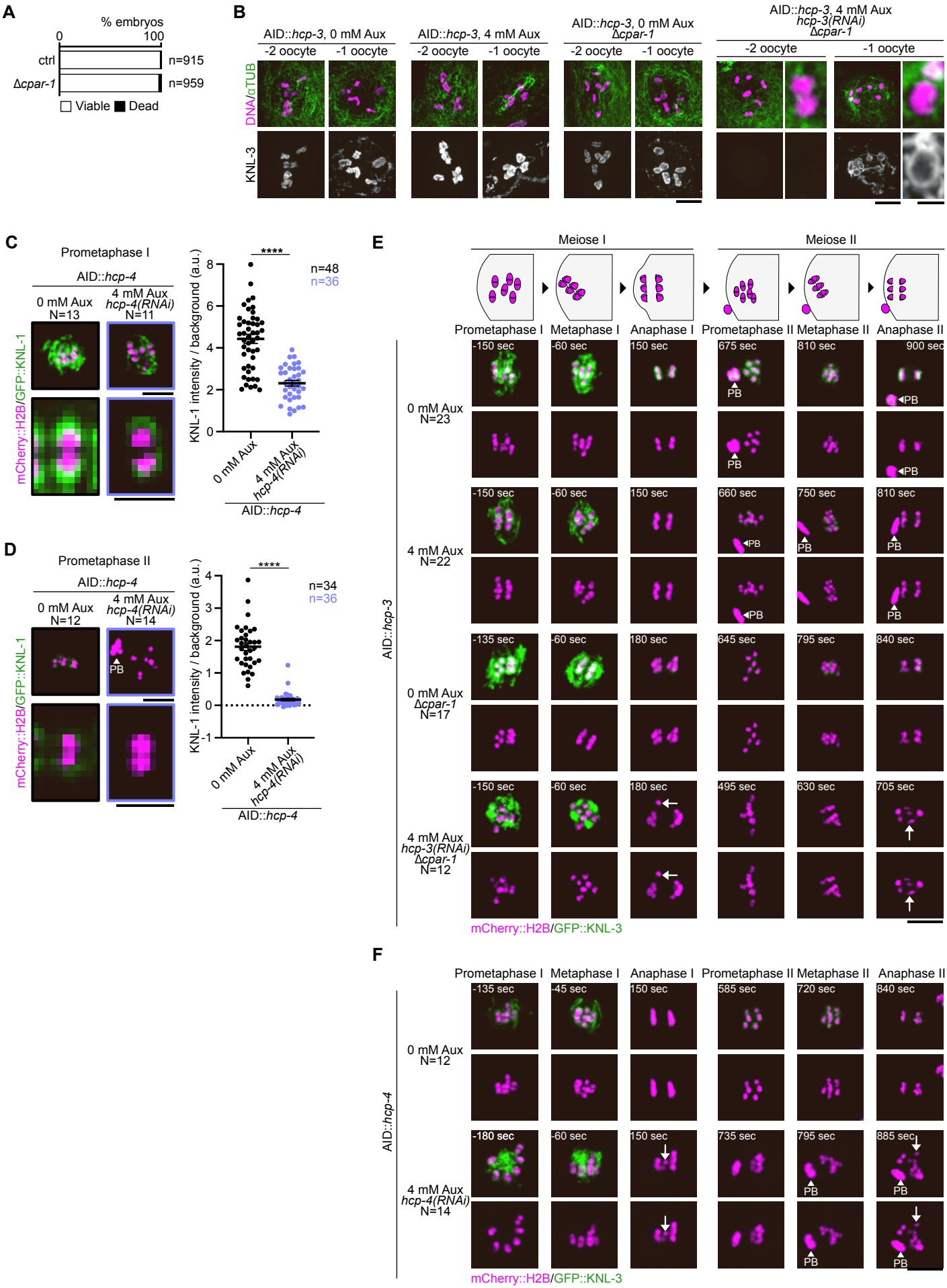
A
% embryos
0
100
ctrl
n=915
Δcpar-1
n=959
Viable
Dead
B
AID::hcp-3, 0 mM Aux
AID::hcp-3, 4 mM Aux
AID::hcp-3, 0 mM Aux Δcpar-1
AID::hcp-3, 4 mM Aux hcp-3(RNAi) Δcpar-1
-2 oocyte
-1 oocyte
DNA/αTUB
KNL-3
C
Prometaphase I
AID::hcp-4
0 mM Aux N=13
4 mM Aux hcp-4(RNAi) N=11
mCherry::H2B/GFP::KNL-1
KNL-1 intensity / background (a.u.)
****
n=48
n=36
0 mM Aux
4 mM Aux hcp-4(RNAi)
AID::hcp-4
D
Prometaphase II
AID::hcp-4
0 mM Aux N=12
4 mM Aux hcp-4(RNAi) N=14
PB
mCherry::H2B/GFP::KNL-1
KNL-1 intensity / background (a.u.)
****
n=34
n=36
0 mM Aux
4 mM Aux hcp-4(RNAi)
AID::hcp-4
E
Meiose I
Meiose II
Prometaphase I
Metaphase I
Anaphase I
Prometaphase II
Metaphase II
Anaphase II
AID::hcp-3
0 mM Aux N=23
4 mM Aux N=22
0 mM Aux Δcpar-1 N=17
4 mM Aux hcp-3(RNAi) Δcpar-1 N=12
-150 sec
-60 sec
150 sec
675 sec
810 sec
900 sec
660 sec
750 sec
-135 sec
180 sec
645 sec
795 sec
840 sec
495 sec
630 sec
705 sec
PB
mCherry::H2B/GFP::KNL-3
F
Prometaphase I
Metaphase I
Anaphase I
Prometaphase II
Metaphase II
Anaphase II
AID::hcp-4
0 mM Aux N=12
4 mM Aux hcp-4(RNAi) N=14
-135 sec
-45 sec
150 sec
585 sec
720 sec
840 sec
-180 sec
-60 sec
735 sec
795 sec
885 sec
PB
mCherry::H2B/GFP::KNL-3

FIGURE S1. Meiotic chromosome segregation defects observed in absence of the CENP-A paralogs or of HCP-4^{CENP-C}. Related to Figure 2.

(A) Embryonic viability assay in control and Δ*cpar-1* mutant worms. Sample size (n embryos). (B) Immunofluorescence images, centered on chromosomes, of oocytes in indicated conditions stained for DNA (magenta), α-tubulin (green), and KNL-3^{DSN1} (grey). Scale bars, 5 μm. (C-D) Left: Representative images of chromosomes in mCherry::HIS-11^{H2B} (magenta) and GFP::KNL-1^{KNL-1} (green) -expressing oocytes in indicated conditions. The white arrowhead indicates the first polar body (PB). Sample sizes (N oocytes). Scale bars, 5 μm. For each condition, bottom: zoom on one homologous chromosome pair (C) or on one sister chromatid pair (D); scale bars, 2 μm. Right: quantification of GFP::KNL-1^{KNL-1} mean intensity at cup-like kinetochores. Error bars, SEM. Sample size (n cup-like kinetochores) is indicated for each condition. Mann-Whitney test, **** $p < 0.0001$. (E-F) Representative time-lapse images of meiosis I and meiosis II of mCherry::HIS-11^{H2B} and GFP::KNL-3 (green) -expressing oocytes in indicated conditions. Time in seconds relative to anaphase I onset. White arrows highlight mis segregating chromosomes. White arrowheads indicate first polar bodies (PB). Sample sizes (N oocytes). Scale bar, 5 μm.

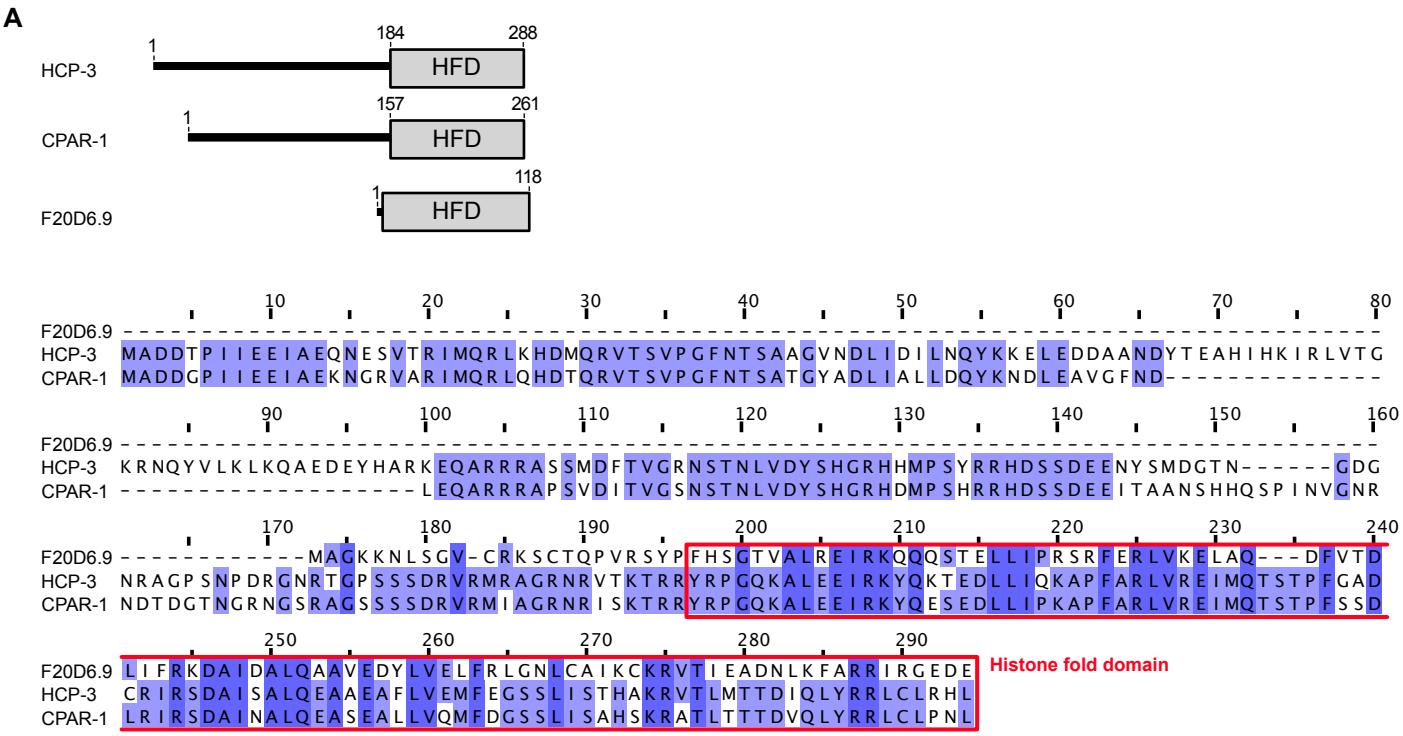
A
HCP-3
CPAR-1
F20D6.9
HFD
1
184
288
157
261
118
Histone fold domain

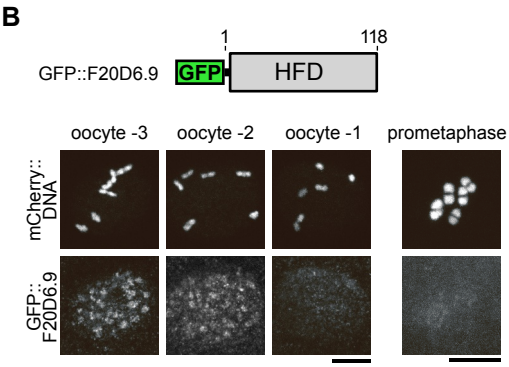
B
GFP::F20D6.9
GFP
HFD
1
118
oocyte -3
oocyte -2
oocyte -1
prometaphase I
mCherry::DNA
GFP::F20D6.9

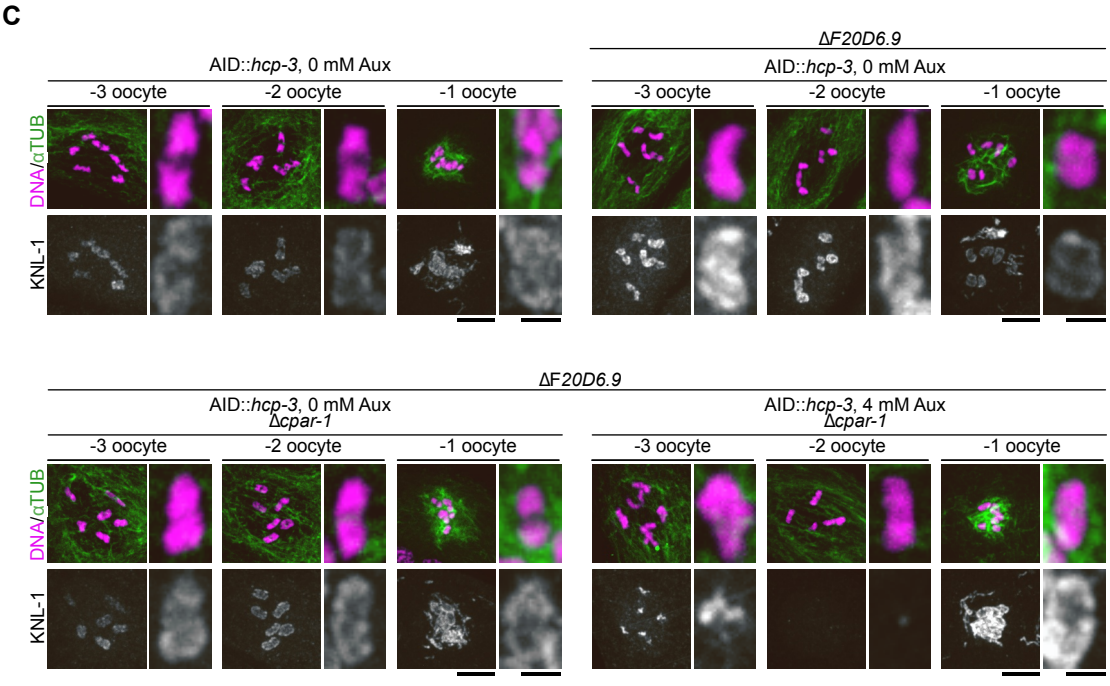
C
AID::hcp-3, 0 mM Aux
ΔF20D6.9
-3 oocyte
-2 oocyte
-1 oocyte
DNA/αTUB
KNL-1
ΔF20D6.9
AID::hcp-3, 0 mM Aux Δcpar-1
AID::hcp-3, 4 mM Aux Δcpar-1

FIGURE S2. The histone H3 variant F20D6.9 is not involved in outer kinetochore assembly in *C. elegans* oocytes. Related to Figure 2.

(A) Top: schematics of the three H3 histone variants HCP-3^{CENP-A}, CPAR-1^{CENP-A} and F20D6.9. Red boxes represent the Histone Fold Domains (HFD). Bottom: protein sequence alignment for HCP-3^{CENP-A}, CPAR-1^{CENP-A} and F20D6.9. Conserved amino acids are highlighted in blue. The red box represents the Histone Fold Domains (HFD). (B) Top: schematic of the GFP::F20D6.9 transgene. Bottom: representative images, centered on chromosomes, of mCherry::HIS-11^{H2B} and GFP::F20D6.9-expressing oocytes. Scale bars, 5 μm. (C) Immunofluorescence images, centered on chromosomes, of oocytes in indicated conditions stained for DNA (magenta), α-tubulin (green) and KNL-1^{KNL1} (grey). Scale bars, 5 μm. For each oocyte, right: zoom on one homologous chromosome pair; scale bars, 1 μm.

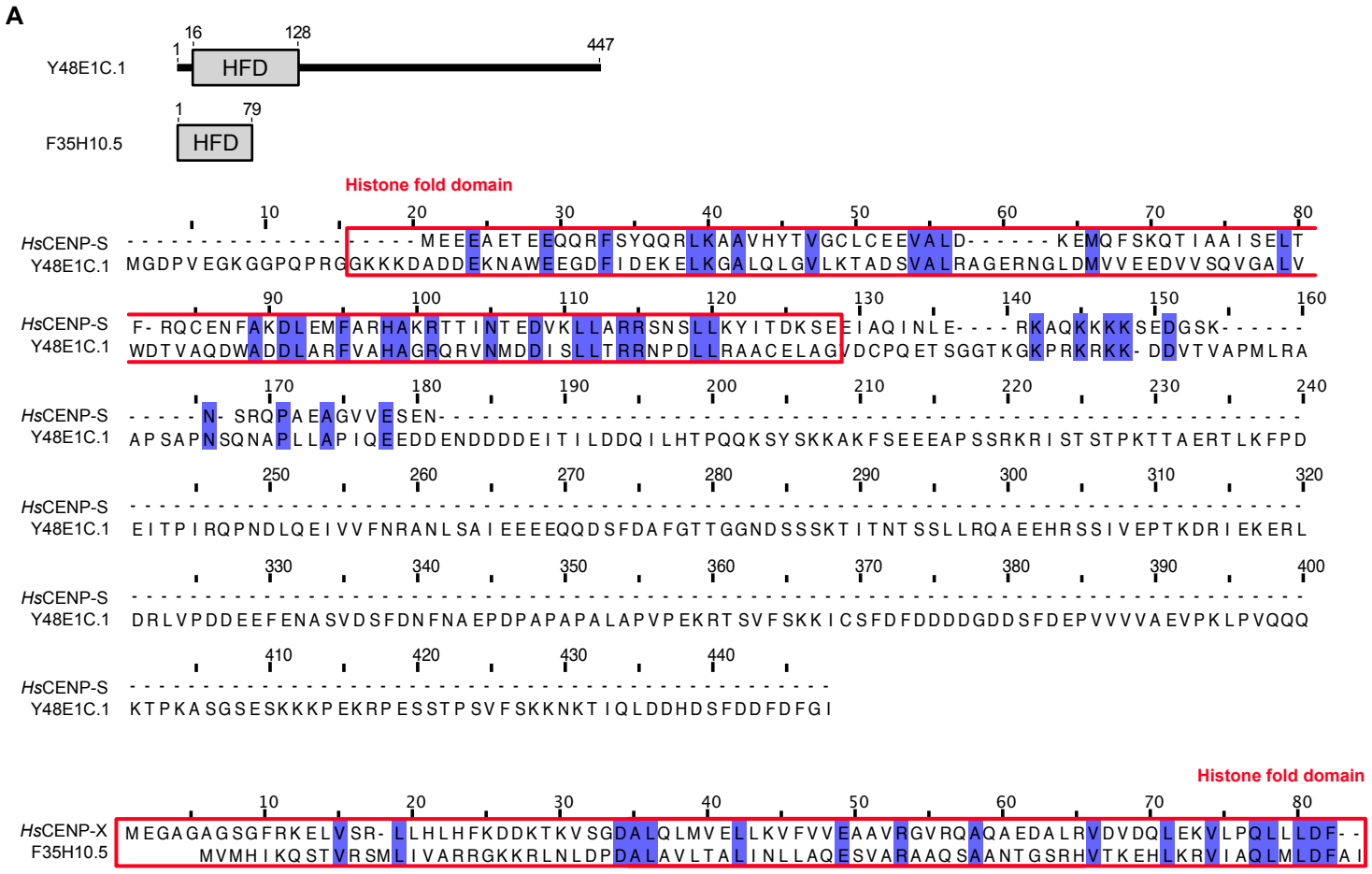
A
Y48E1C.1
HFD
F35H10.5
HFD
Histone fold domain
HsCENP-S
Y48E1C.1
HsCENP-S
Y48E1C.1
HsCENP-S
Y48E1C.1
HsCENP-S
Y48E1C.1
HsCENP-S
Y48E1C.1
Histone fold domain
HsCENP-X
F35H10.5

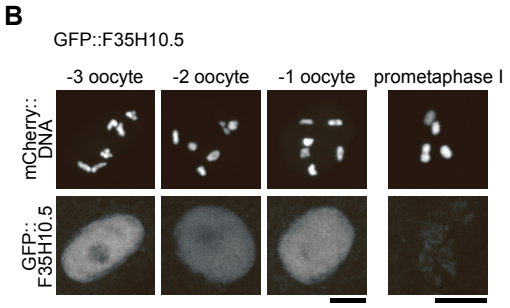
B
GFP::F35H10.5
-3 oocyte
-2 oocyte
-1 oocyte
prometaphase I
mCherry::DNA
GFP::F35H10.5

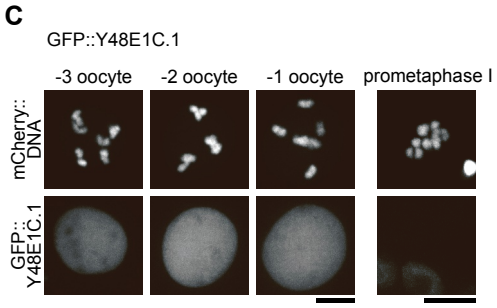
C
GFP::Y48E1C.1
-3 oocyte
-2 oocyte
-1 oocyte
prometaphase I
mCherry::DNA
GFP::Y48E1C.1

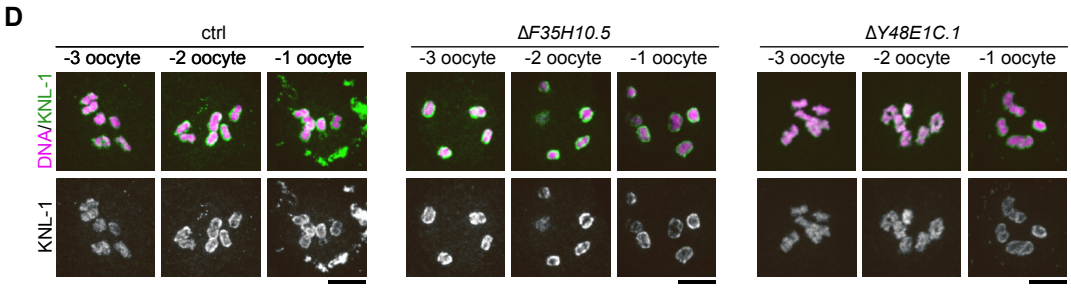
D
ctrl
ΔF35H10.5
ΔY48E1C.1
-3 oocyte
-2 oocyte
-1 oocyte
DNA/KNL-1
KNL-1

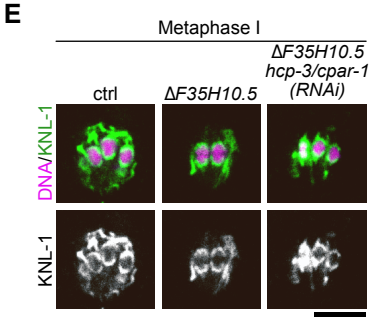
E
Metaphase I
ctrl
ΔF35H10.5
ΔF35H10.5 hcp-3/cpar-1 (RNAi)
DNA/KNL-1
KNL-1

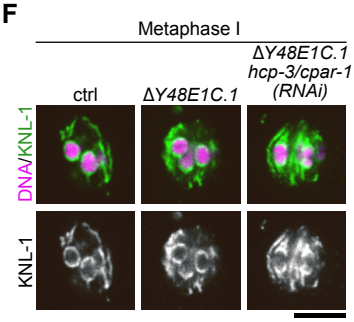
F
Metaphase I
ctrl
ΔY48E1C.1
ΔY48E1C.1 hcp-3/cpar-1 (RNAi)
DNA/KNL-1
KNL-1

FIGURE S3. The CCAN components Y48E1C.1^{CENP-S} and F35H10.5^{CENP-X} are not involved in outer kinetochore assembly in *C. elegans* oocytes. Related to Figure 2.

(A) Top: schematics of the CCAN components Y48E1C.1^{CENP-S} and F35H10.5^{CENP-X}. Bottom: protein sequence alignment between *Hs*CENP-S and Y48E1C.1^{CENP-S}, and between *Hs*CENP-X and F35H10.5^{CENP-X}. Conserved amino acids are highlighted in blue. Red boxes represent the Histone Fold Domains (HFD). (B-C) Representative images, centered on chromosomes, of mCherry::HIS-11^{H2B} and GFP:: Y48E1C.1^{CENP-S} (B) or GFP:: F35H10.5^{CENP-X} (C) -expressing oocytes. Scale bars, 5 μm. (D-F) Immunofluorescence images, centered on chromosomes, of oocytes in indicated conditions stained for DNA (magenta) and KNL-1^{KNL1} (green). Scale bars, 5 μm.

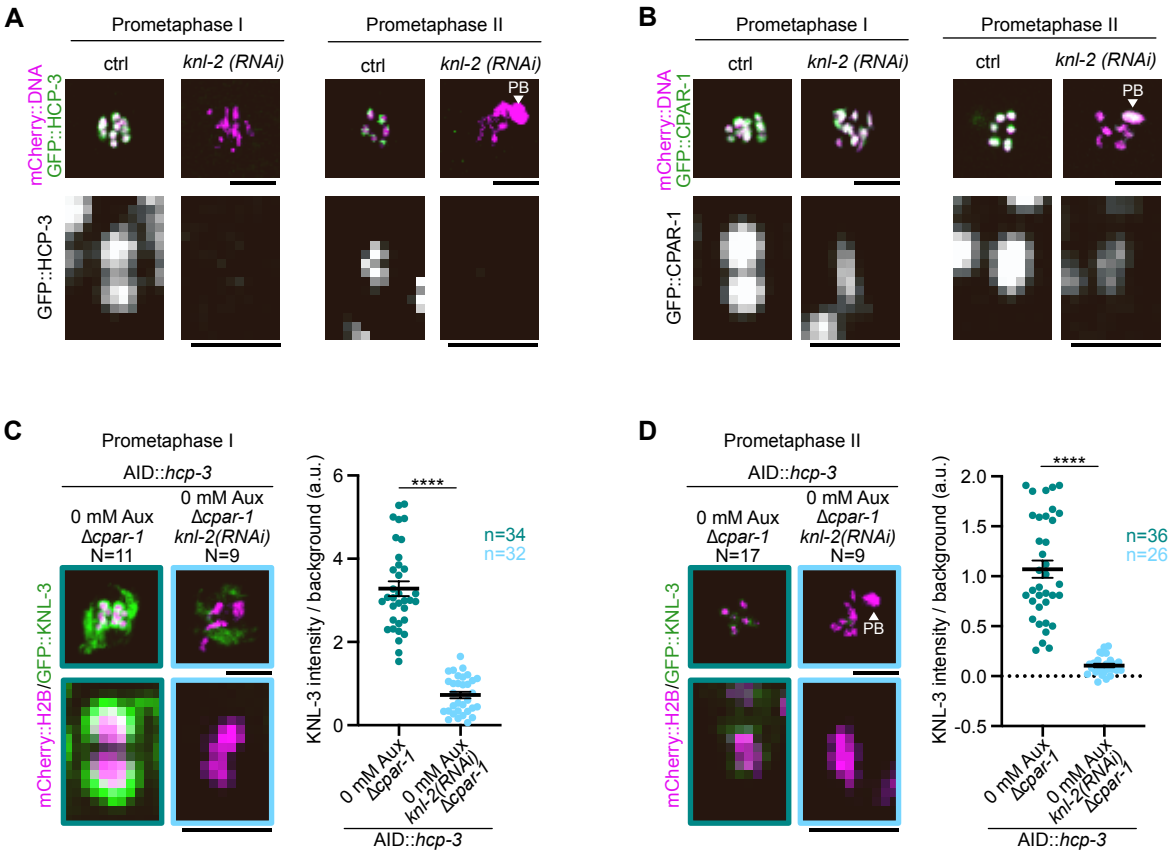
A
Prometaphase I
Prometaphase II
ctrl
knl-2 (RNAi)
ctrl
knl-2 (RNAi)
mCherry::DNA
GFP::HCP-3
PB
GFP::HCP-3
B
Prometaphase I
Prometaphase II
ctrl
knl-2 (RNAi)
ctrl
knl-2 (RNAi)
mCherry::DNA
GFP::CPAR-1
PB
GFP::CPAR-1
C
Prometaphase I
AID::hcp-3
0 mM Aux
Δcpar-1
N=11
0 mM Aux
Δcpar-1
knl-2(RNAi)
N=9
mCherry::H2B/GFP::KNL-3
KNL-3 intensity / background (a.u.)
6
4
2
0
****
n=34
n=32
0 mM Aux Δcpar-1
0 mM Aux knl-2(RNAi) Δcpar-1
AID::hcp-3
D
Prometaphase II
AID::hcp-3
0 mM Aux
Δcpar-1
N=17
0 mM Aux
Δcpar-1
knl-2(RNAi)
N=9
mCherry::H2B/GFP::KNL-3
PB
KNL-3 intensity / background (a.u.)
2.0
1.5
1.0
0.5
0.0
-0.5
****
n=36
n=26
0 mM Aux Δcpar-1
0 mM Aux knl-2(RNAi) Δcpar-1
AID::hcp-3

FIGURE S4. Function of KNL-2^{M18BP1} in HCP-3^{CENP-A} and CPAR-1^{CENP-1} localizations and in outer kinetochore assembly during the meiotic divisions. Related to Figure 3.

(A-B) Representative images of chromosomes in mCherry::HIS-11^{H2B} (magenta) and GFP::HCP-3^{CENP-A} (green, A) or GFP::CPAR-1^{CENP-A} (green, B) -expressing oocytes in indicated conditions. White arrowheads indicate first polar bodies (PB). Scale bars, 5 μm. For each condition, bottom: zoom on one homologous chromosome pair (Prometaphase I) or on one sister chromatid pair (Prometaphase II); scale bars, 2 μm. (C-D) Left: representative images of chromosomes in mCherry::HIS-11^{H2B} (magenta) and GFP::KNL-3^{DSN1} (green) -expressing oocytes in indicated conditions. White arrowheads indicate first polar body (PB). Sample sizes (N oocytes). Scale bar, 5 μm. For each condition, bottom: zoom on one homologous chromosome pair (A) or on one sister chromatid pair (B); scale bar, 2 μm. Right: quantification of GFP::KNL-3^{DSN1} mean intensity at cup-like kinetochores. Error bars, SEM. Sample size (n cup-like kinetochores) is indicated for each condition. Mann-Whitney test test, **** $p < 0.0001$.

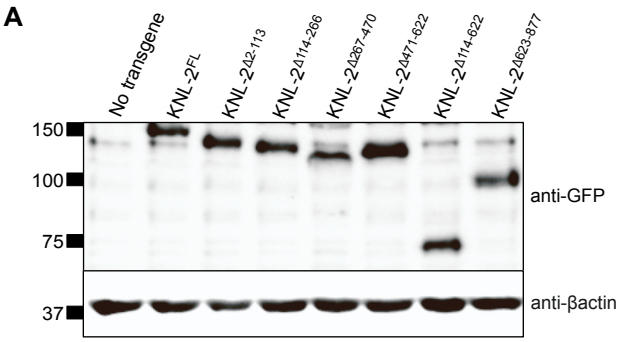
A
No transgene
KNL-2FL
KNL-2Δ2-113
KNL-2Δ114-266
KNL-2Δ267-470
KNL-2Δ471-622
KNL-2Δ114-622
KNL-2Δ623-877
150
100
75
37
anti-GFP
anti-βactin

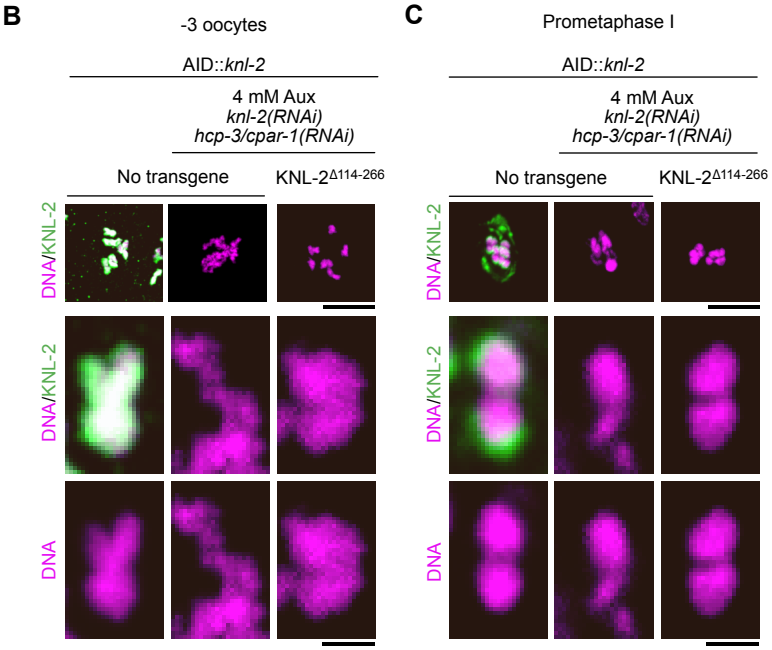
B
-3 oocytes
AID::knl-2
4 mM Aux
knl-2(RNAi)
hcp-3/cpar-1(RNAi)
No transgene
KNL-2Δ114-266
DNA/KNL-2
DNA/KNL-2
DNA
C
Prometaphase I
AID::knl-2
4 mM Aux
knl-2(RNAi)
hcp-3/cpar-1(RNAi)
No transgene
KNL-2Δ114-266
DNA/KNL-2
DNA/KNL-2
DNA

FIGURE S5. The KNL-2^{M18BP1} N-terminal domain is required for KNL-2^{M18BP1} localization at cup-like kinetochores. Related to Figure 4.

(A) Western blot of full-worm protein extracts (100 worms per lane) in indicated conditions using an anti-GFP antibody for transgene detection, and an anti-βactin as a loading control. (B-C) Top: representative images of diakinesis -3 oocytes (B) and prometaphase I oocytes (C) in control (No transgene) or GFP::KNL-2$^{\Delta 114\text{-}266}$-expressing oocytes in indicated conditions stained for DNA (magenta) and KNL-2^{M18BP1} (green). Scale bar, 5 μm. For each condition, bottom: zoom on one homologous chromosome (B) or sister chromatid pair (C); scale bar, 1 μm.

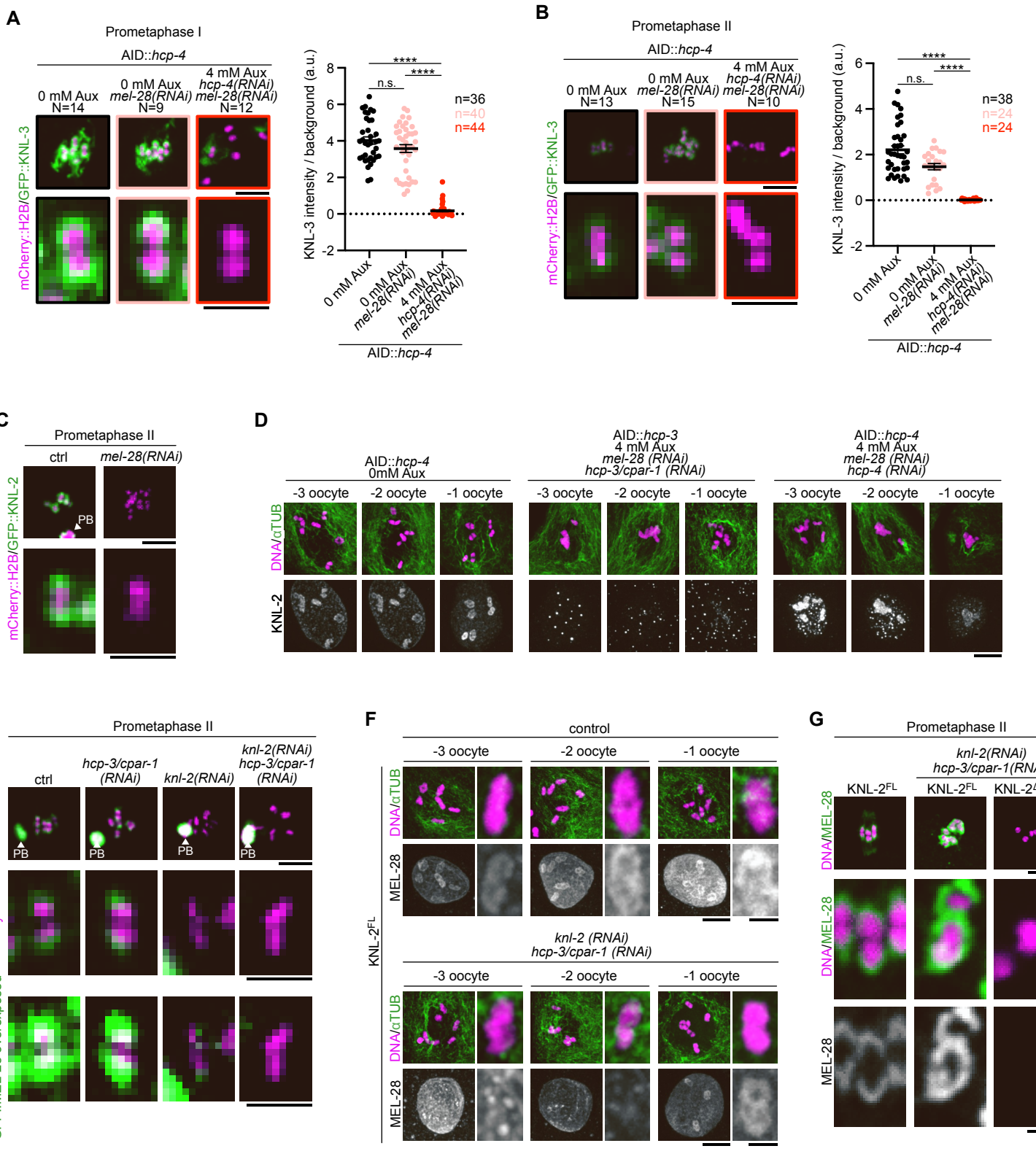
A
Prometaphase I
AID::hcp-4
0 mM Aux N=14
0 mM Aux mel-28(RNAi) N=9
4 mM Aux hcp-4(RNAi) mel-28(RNAi) N=12
mCherry::H2B/GFP::KNL-3
KNL-3 intensity / background (a.u.)
n.s.
****
****
n=36
n=40
n=44
0 mM Aux
0 mM Aux mel-28(RNAi)
4 mM Aux hcp-4(RNAi) mel-28(RNAi)
AID::hcp-4
B
Prometaphase II
AID::hcp-4
0 mM Aux N=13
0 mM Aux mel-28(RNAi) N=15
4 mM Aux hcp-4(RNAi) mel-28(RNAi) N=10
mCherry::H2B/GFP::KNL-3
KNL-3 intensity / background (a.u.)
n.s.
****
****
n=38
n=24
n=24
0 mM Aux
0 mM Aux mel-28(RNAi)
4 mM Aux hcp-4(RNAi) mel-28(RNAi)
AID::hcp-4
C
Prometaphase II
ctrl
mel-28(RNAi)
PB
mCherry::H2B/GFP::KNL-2
D
AID::hcp-4 0mM Aux
AID::hcp-3 4 mM Aux mel-28 (RNAi) hcp-3/cpar-1 (RNAi)
AID::hcp-4 4 mM Aux mel-28 (RNAi) hcp-4 (RNAi)
-3 oocyte
-2 oocyte
-1 oocyte
DNA/αTUB
KNL-2
E
Prometaphase II
ctrl
hcp-3/cpar-1 (RNAi)
knl-2(RNAi)
knl-2(RNAi) hcp-3/cpar-1 (RNAi)
PB
mCherry::H2B/GFP::MEL-28
mCherry::H2B/ GFP::MEL-28 overexposed
F
control
-3 oocyte
-2 oocyte
-1 oocyte
DNA/αTUB
MEL-28
KNL-2FL
knl-2 (RNAi) hcp-3/cpar-1 (RNAi)
G
Prometaphase II
knl-2(RNAi) hcp-3/cpar-1(RNAi)
KNL-2FL
KNL-2FL
KNL-2Δ114-266
PB
DNA/MEL-28
MEL-28

FIGURE S6. Interdependency between KNL-2^{M18BP1} and MEL-28^{ELYS} for their chromosomal localizations in *C. elegans* oocytes. Related to Figure 5.

(A-B) Representative images of chromosomes in mCherry::HIS-11^{H2B} (magenta) and GFP::KNL-3^{DSN1} (green)-expressing oocytes in indicated conditions. Sample sizes (N oocytes). Scale bars, 5 μm. For each condition, bottom: zoom on one homologous chromosome pair (A) or on one sister chromatid pair (B); scale bar, 2 μm. Right: quantification of GFP::KNL-3^{DSN1} mean intensity at cup-like kinetochores. Error bars, SEM. Sample size (n cup-like kinetochores) is indicated for each condition. Kruskal-Wallis one-way ANOVA test **** $p < 0.0001$, n.s. not significant. (C) Representative images of chromosomes in mCherry::HIS-11^{H2B} (magenta) and GFP::KNL-2^{M18BP1} (green)-expressing oocytes in indicated conditions. The white arrowhead indicates the first polar body (PB). Scale bar, 5 μm. For each condition, bottom: zoom on one sister chromatid pair; scale bar, 2 μm. (D) Immunofluorescence images, centered on chromosomes, of oocytes in indicated conditions stained for DNA (magenta), α-tubulin (green) and KNL-2^{M18BP1} (grey). Scale bar, 5 μm. (E) Representative images of chromosomes in mCherry::HIS-11^{H2B} (magenta) and GFP::MEL-28^{ELYS} (green)-expressing oocytes in indicated conditions. White arrowheads indicate first polar bodies (PB). Scale bar, 5 μm. For each condition, bottom: zoom on one sister chromatid pair; scale bar, 2 μm. (F) Immunofluorescence images, centered on chromosomes, of oocytes in indicated conditions stained for DNA (magenta), α-tubulin (green) and MEL-28^{ELYS} (grey). Scale bars, 5 μm. For each oocyte, right: zoom on one homologous chromosome pair; scale bars, 1 μm. (G) Immunofluorescence images, centered on chromosomes, of oocytes in indicated conditions stained for DNA (magenta) and MEL-28^{ELYS} (green). The white arrowhead indicates the first polar body (PB). Scale bar, 5 μm. For each condition, bottom: zoom on one sister chromatid pair; scale bar, 1 μm.